The First (and last) Billion Years of Star Formation in the Universe

Avi Loeb

Harvard University

Collaborators: ***R. Barkana, TJ Cox, S.Wyithe, M. Zaldarriaga***

Star Formation Through Cosmic Time, August 13-17, 2007

THE DARK AGES of the Universe

Astronomers are trying to fill in the blank pages in our photo album of the infant universe

By Abraham Loeb

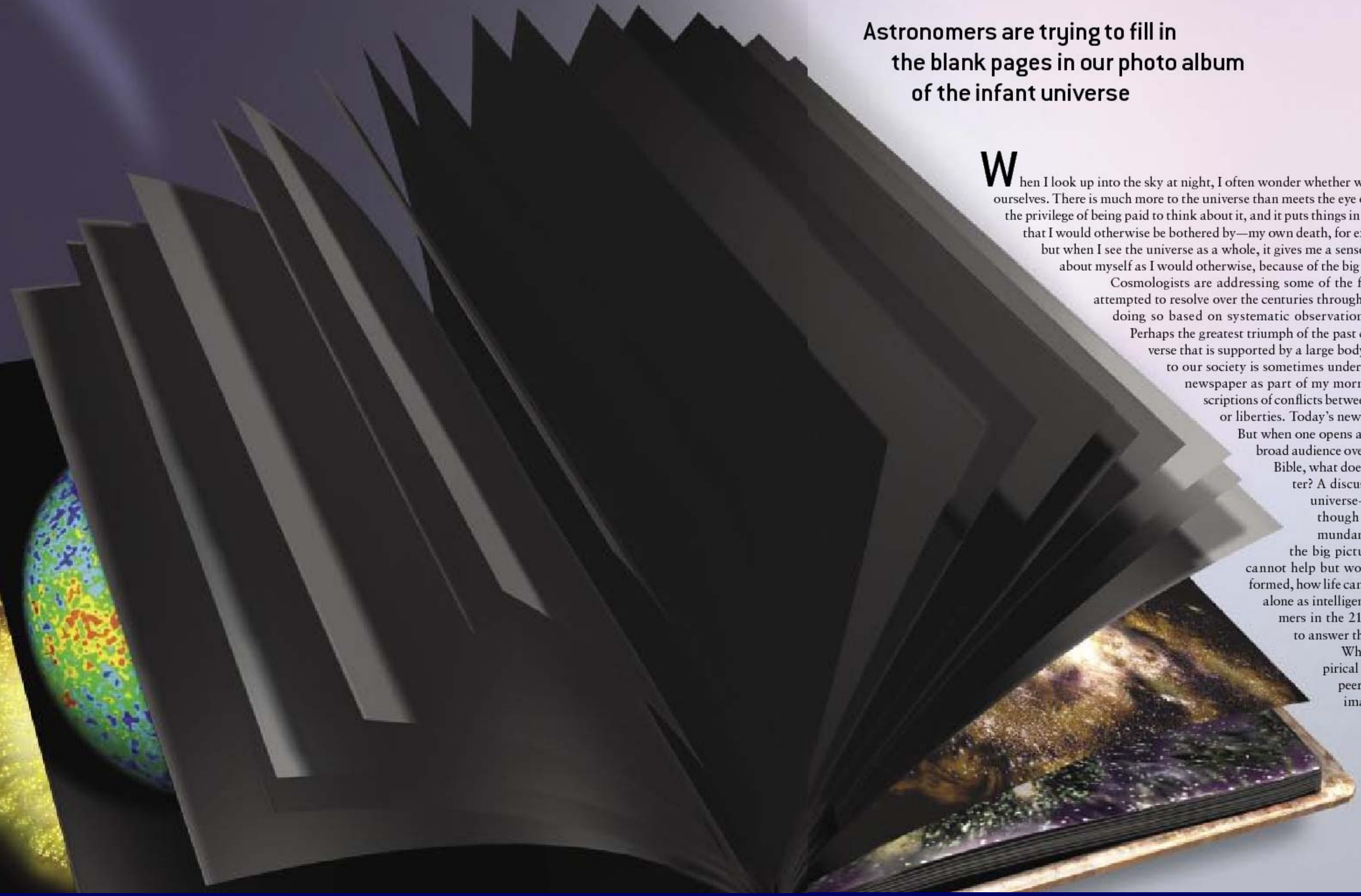

When I look up into the sky at night, I often wonder whether we humans are too preoccupied with ourselves. There is much more to the universe than meets the eye on earth. As an astrophysicist I have the privilege of being paid to think about it, and it puts things in perspective for me. There are things that I would otherwise be bothered by—my own death, for example. Everyone will die sometime, but when I see the universe as a whole, it gives me a sense of longevity. I do not care so much about myself as I would otherwise, because of the big picture.

Cosmologists are addressing some of the fundamental questions that people attempted to resolve over the centuries through philosophical thinking, but we are doing so based on systematic observation and a quantitative methodology. Perhaps the greatest triumph of the past century has been a model of the universe that is supported by a large body of data. The value of such a model to our society is sometimes underappreciated. When I open the daily newspaper as part of my morning routine, I often see lengthy descriptions of conflicts between people about borders, possessions or liberties. Today's news is often forgotten a few days later. But when one opens ancient texts that have appealed to a broad audience over a longer period of time, such as the Bible, what does one often find in the opening chapter? A discussion of how the constituents of the universe—light, stars, life—were created. Although humans are often caught up with mundane problems, they are curious about the big picture. As citizens of the universe we cannot help but wonder how the first sources of light formed, how life came into existence and whether we are alone as intelligent beings in this vast space. Astronomers in the 21st century are uniquely positioned to answer these big questions.

What makes modern cosmology an empirical science is that we are literally able to peer into the past. When you look at your image reflected off a mirror one meter

On small scales the universe is clumpy

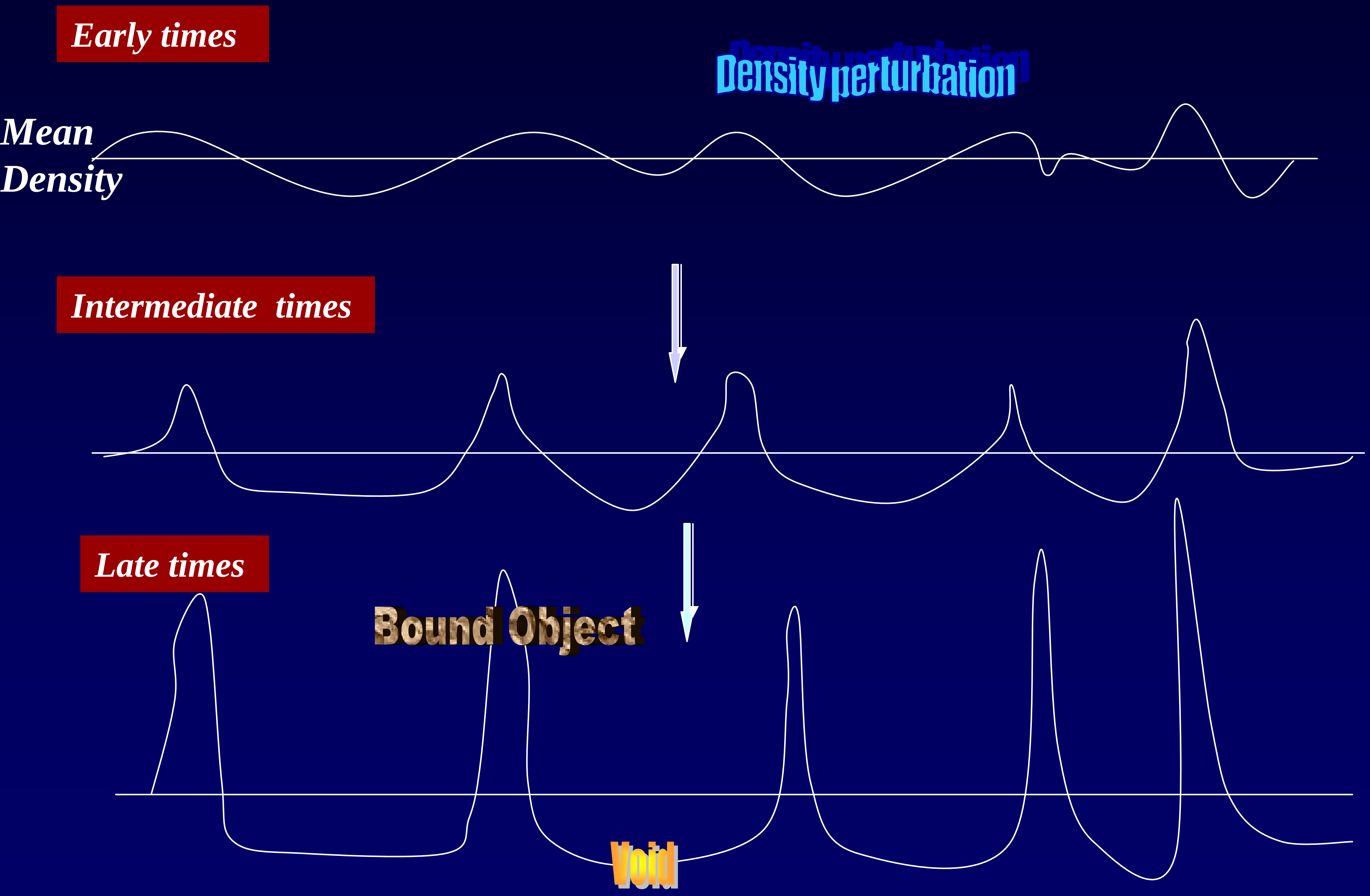

Current Composition of the Universe

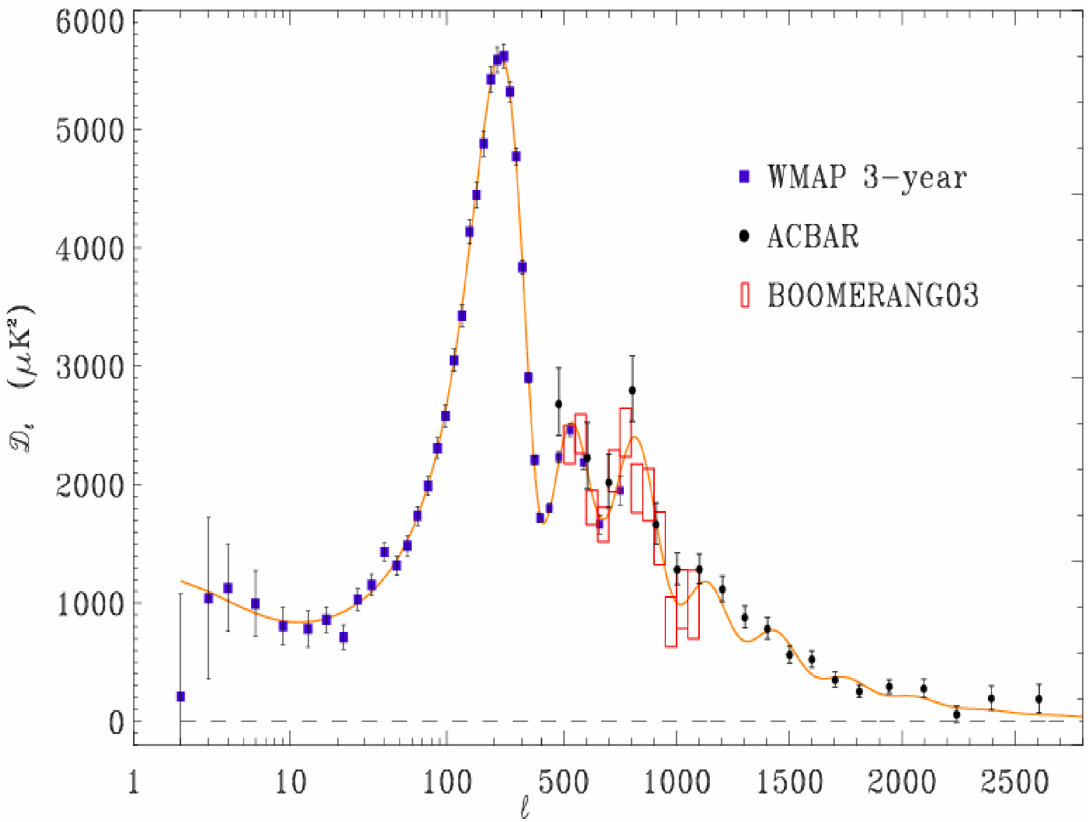

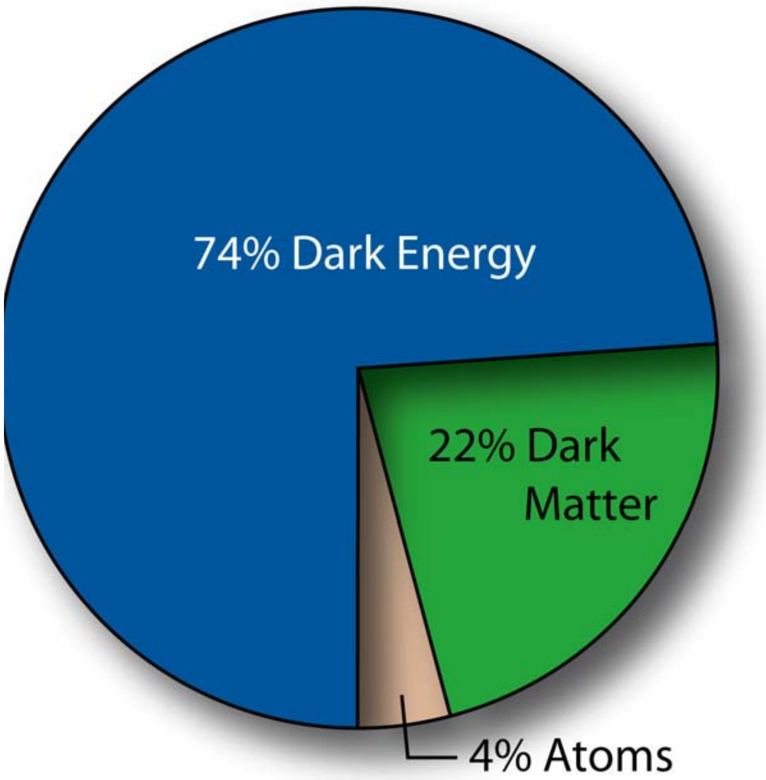

Silk damping of small-scale fluctuatons in the baryon-photon fluid prior to cosmic recombination implies that galaxies could not have formed in our Universe without dark matter!

The First Dark Matter Objects in the Universe

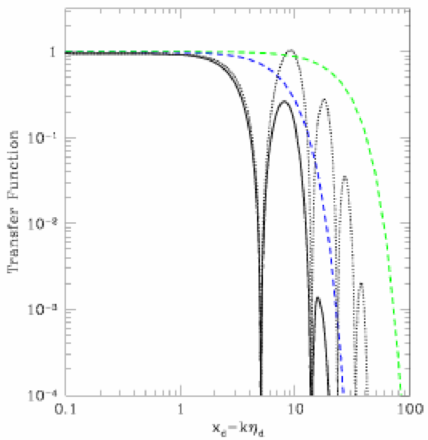

Transfer function of the CDM density perturbation amplitude (normalized by the primordial amplitude from inflation). We show two cases: *(i)* $T_d/M = 10^{-4}$ and $T_d/T_{eq} = 10^7$; *(ii)* $T_d/M = 10^{-5}$ and $T_d/T_{eq} = 10^7$. In each case the oscillatory curve is our result and the other curve is the free-streaming only result that was derived previously in the literature [4,7,8].

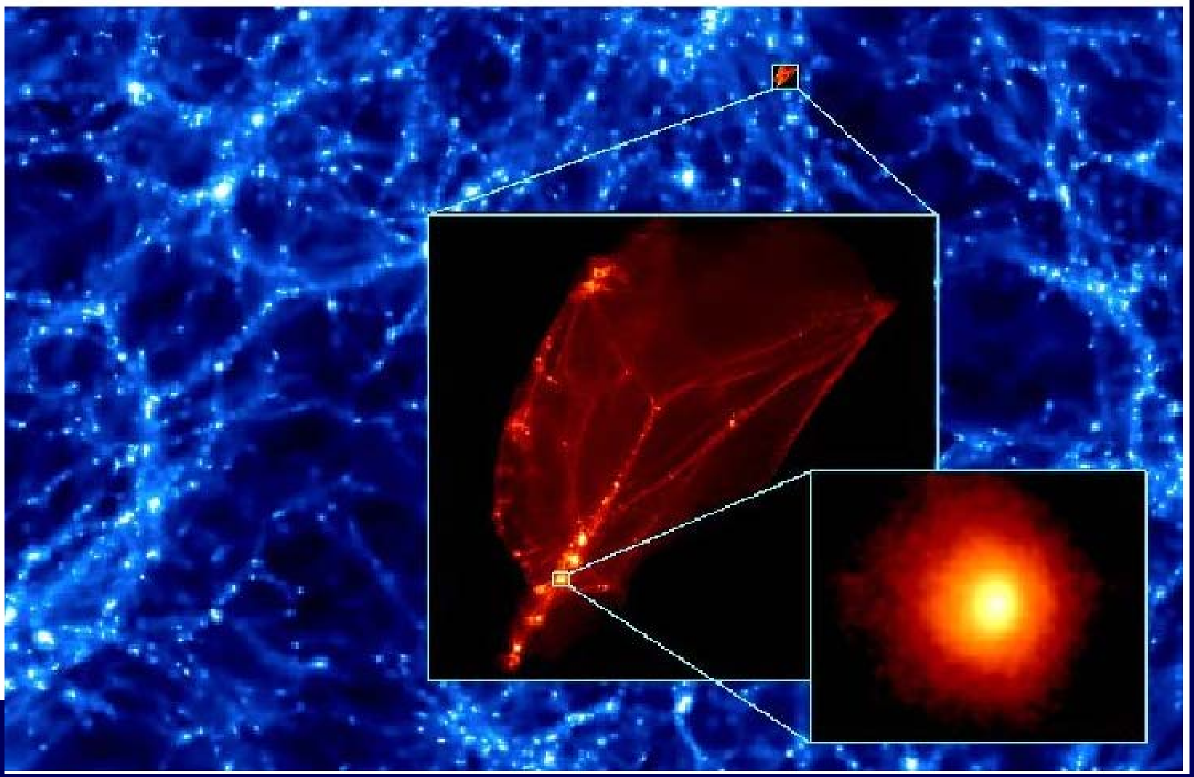

Smallest dark matter clumps: ~0.1 Jupiter mass

$$M_{\rm cut} = \frac{4\pi}{3}\left(\frac{\pi}{k_{\rm cut}}\right)^3 \Omega_M \rho_{\rm crit} \simeq 10^{-4}\left(\frac{T_d}{10\ {\rm MeV}}\right)^{-3} M_\odot,$$

Loeb & Zaldarriaga, astro-ph/0504112

Diemand, Moore & Stadel astro-ph/0501589

Emergence of the First Star Clusters

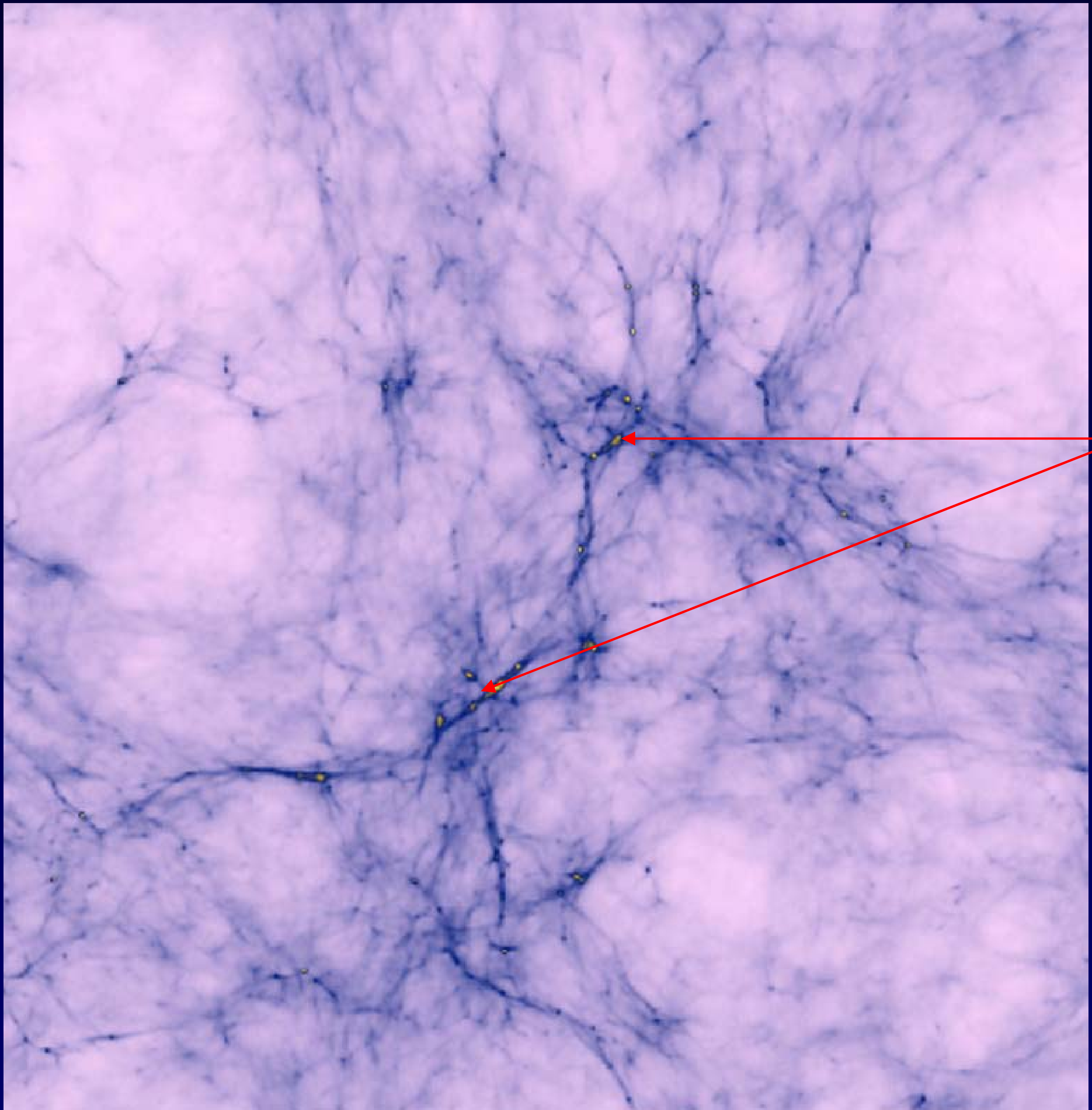

molecular hydrogen in Jeans mass objects

(ø 10^5M ì)

Yoshida et al. 2003

Observing the Cosmic Hydrogen

Hydrogen

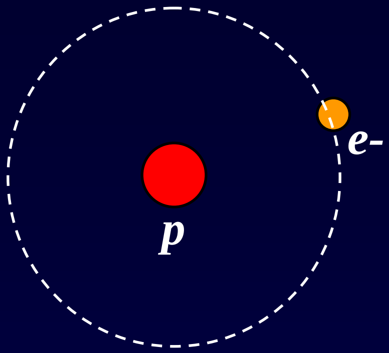

Ground level

excitation rate= (atomic collisions)+(radiative coupling to CMB)

Couple T_s ***to*** T_k ***Couples*** T_s ***to*** $T_{í}$

spin

$$21\text{cm} = (1:4\text{GHz})^{à1}$$

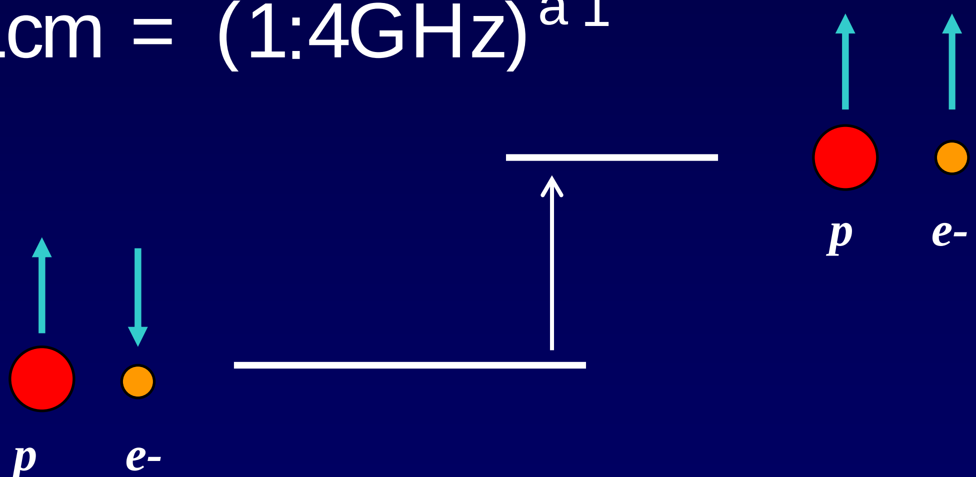

${}_1S_{1=2}$

${}_0S_{1=2}$

Spin Temperature $\frac{n_1}{n_0} = \frac{g_1}{g_0}\,\text{expf}\,à\,\frac{0:068\text{K}}{T_s}\text{g}$ $(g_1=g_0) = 3$

Predicted by Van de Hulst in 1944; Observed by Ewen &Purcell in 1951 at Harvard

Thermal History

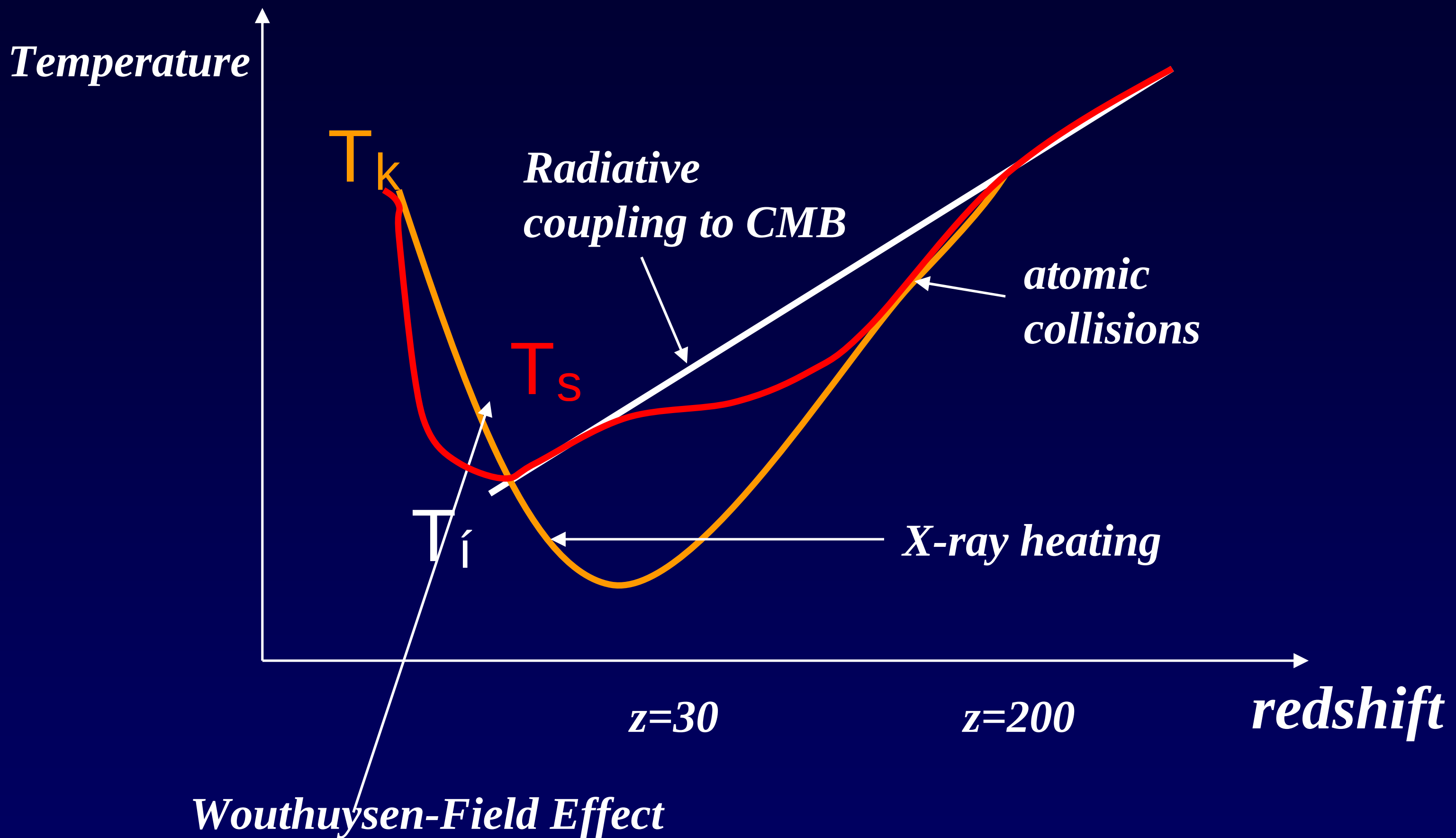

Sources of 21cm fluctuations

Density inhomogeneties (Loeb & Zaldarriaga 04) and peculiar velocities (Barkana & Loeb 04)
Ionized bubbles (Madau,Meiksin &Rees 1997;Furlanetto et al. 2004; Gnedin & Shaver 2003)
Emision from mini-halos (Iliev, Shapiro, et al. 2002)
Fluctuations in Lya flux, and gas temperature (Barkana & Loeb 2004)

LIGHTING UP THE COSMOS

In the beginning of the Dark Ages, electrically neutral hydrogen gas filled the universe. As stars formed, they ionized the regions immediately around them, creating bubbles here and there. Eventually these bubbles merged together, and intergalactic gas became entirely ionized.

Time:	210 million years	290 million years	370 million years	460 million years	540 million years	620 million years	710 million years
Width of frame:	2.4 million light-years	3.0 million light-years	3.6 million light-years	4.1 million light-years	4.6 million light-years	5.0 million light-years	5.5 million light-y
Observed wavelength:	4.1 meters	3.3 meters	2.8 meters	2.4 meters	2.1 meters	2.0 meters	1.8 meters
	All the gas is neutral. The white areas are the densest and will give rise to the first stars and quasars.	Faint red patches show that the stars and quasars have begun to ionize the gas around them.	These bubbles of ionized gas grow.	New stars and quasars form and create their own bubbles.	The bubbles are beginning to interconnect.	The bubbles have merged and nearly taken over all of space.	The only remainin neutral hydrogen is concentrated in galaxies.

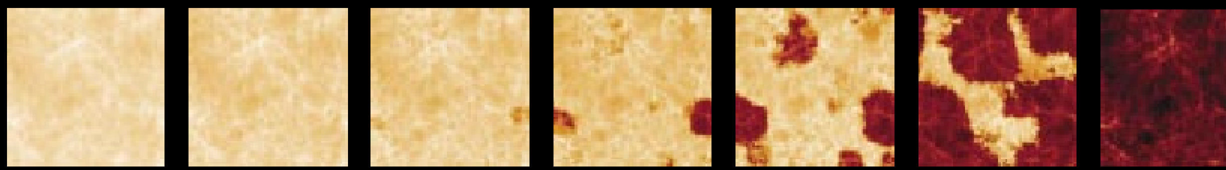

Simulated images of 21-centimeter radiation show how hydrogen gas turns into a galaxy cluster. The amount of radiation (*white is highest; orange and red are intermediate; black is least*) reflects both the density of the gas and its degree of ionization: dense, electrically neutral gas appears white; dense, ionized gas appears black. The images have been rescaled to remove the effect of cosmic expansion and thus highlight the cluster-forming processes. Because of expansion, the 21-centimeter radiation is actually observed at a longer wavelength; the earlier the image, the longer the wavelength.

21 cm Absorption by Hydrogen Prior to Structure Formation

$$T_b = \text{ü} \, \breve{} \, \frac{T_s \text{à} T_{\text{í}}}{1+z} \, ''$$

$$T_b = 28\text{mK} \; \text{a}\frac{1+z}{10}\text{a}^{1=2} \, \breve{} \, \frac{T_s \text{à} T_{\text{í}}}{T_s} \, ''$$

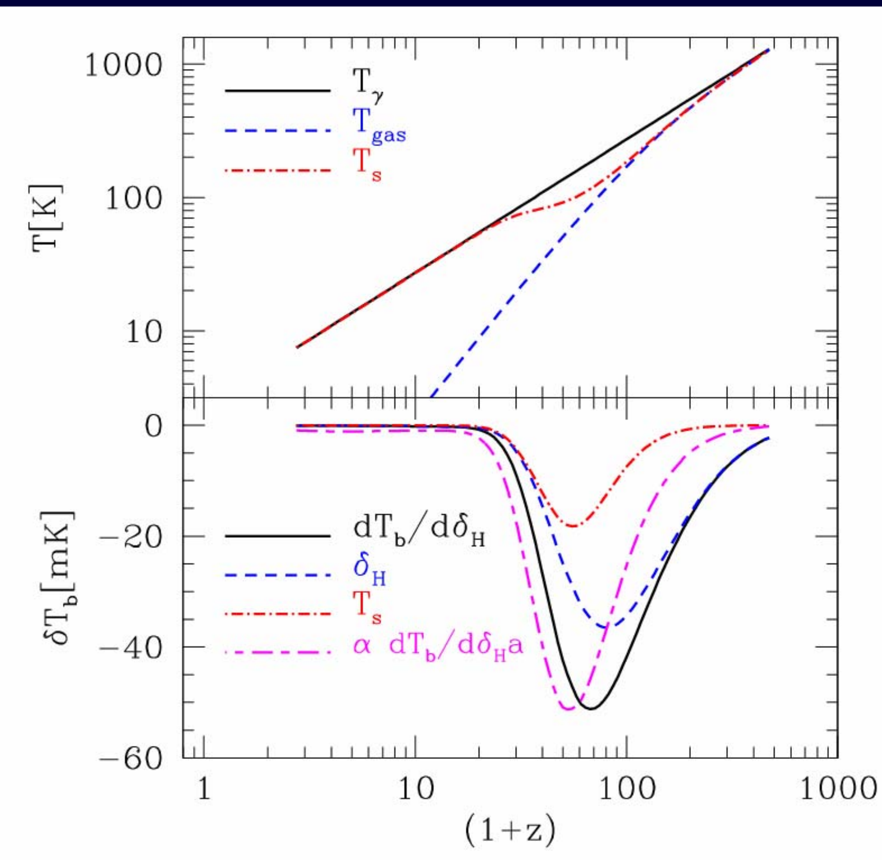

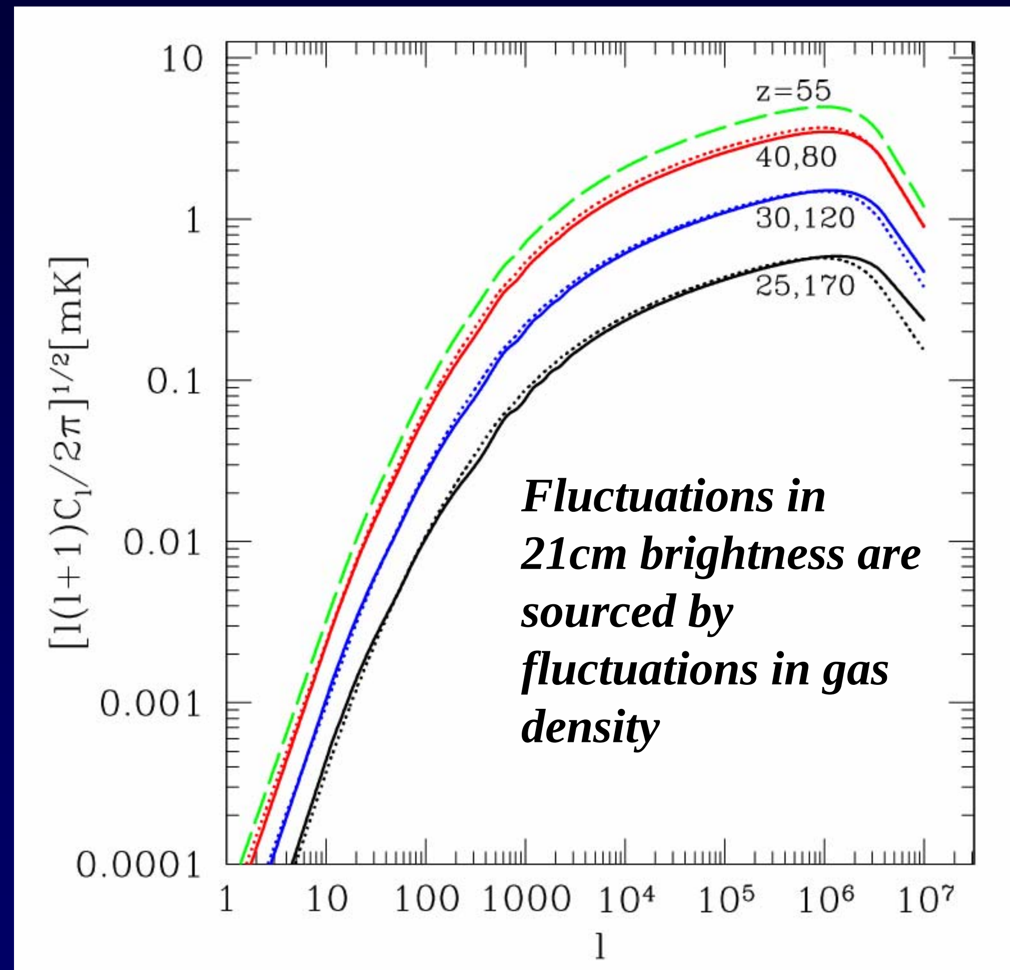

Loeb & Zaldarriaga, Phys. Rev. Lett., 2004; Scott & Rees, MNRAS, 1990

Observed wavelength=21cm (1+z) → 3D tomography (slicing the universe in redshift)

Largest Data Set on the Sky

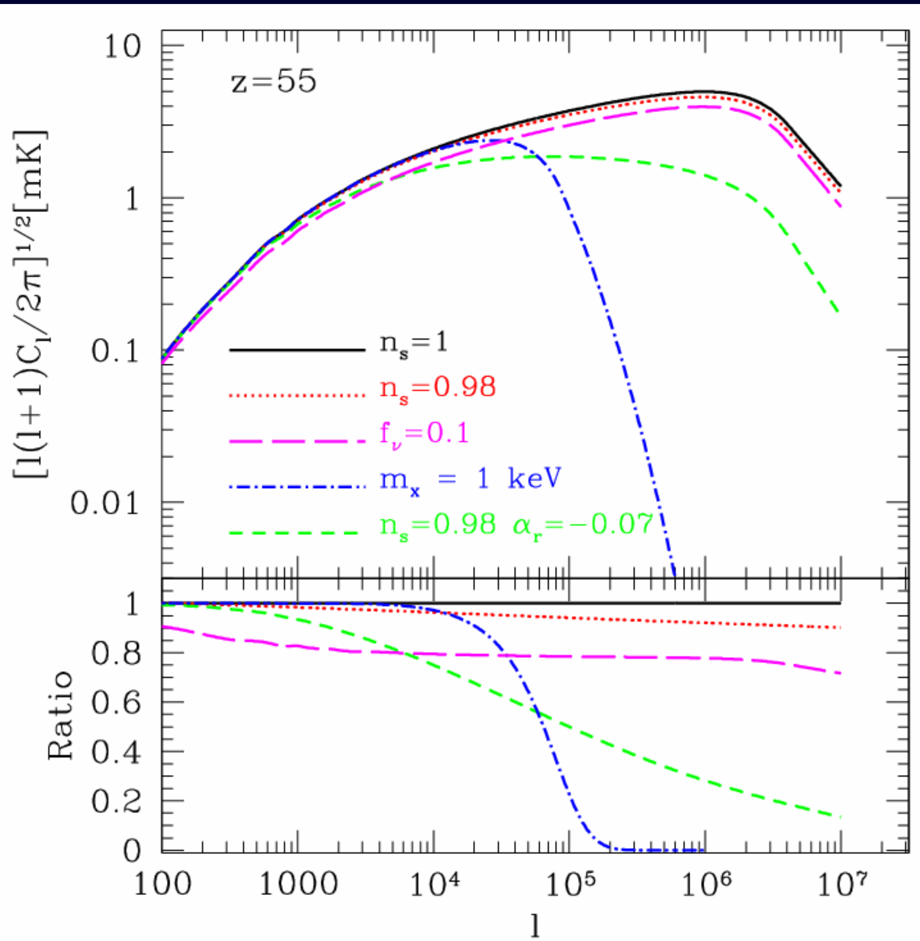

Number of independent patches:

$$\sim 10^{16}\left(\frac{l_{max}}{10^6}\right)^3$$

while Silk damping limits the primary CMB anisotropies to only $\sim 10^7$

Noise due to foreground sky brightness:

$$N_\nu \sim 0.4\ \mathrm{mK}\left(\frac{I_\nu}{5\times 10^5\ \mathrm{Jy\ sr^{-1}}}\right)\left(\frac{l_{min}}{35}\right)\left(\frac{5000}{l_{max}}\right)\left(\frac{0.016}{f_{cover}}\right)\times\left(\frac{1\ \mathrm{year}}{t_0}\right)^{1/2}\left(\frac{\Delta\nu}{\nu}\right)^{-1/2}\left(\frac{50\ \mathrm{MHz}}{\nu}\right)^{5/2},$$

Loeb & Zaldarriaga, Phys. Rev. Lett., 2004; astro-ph/0312134

21cm Tomography of Ionized Bubbles During Reionization is like

Slicing Swiss Cheese

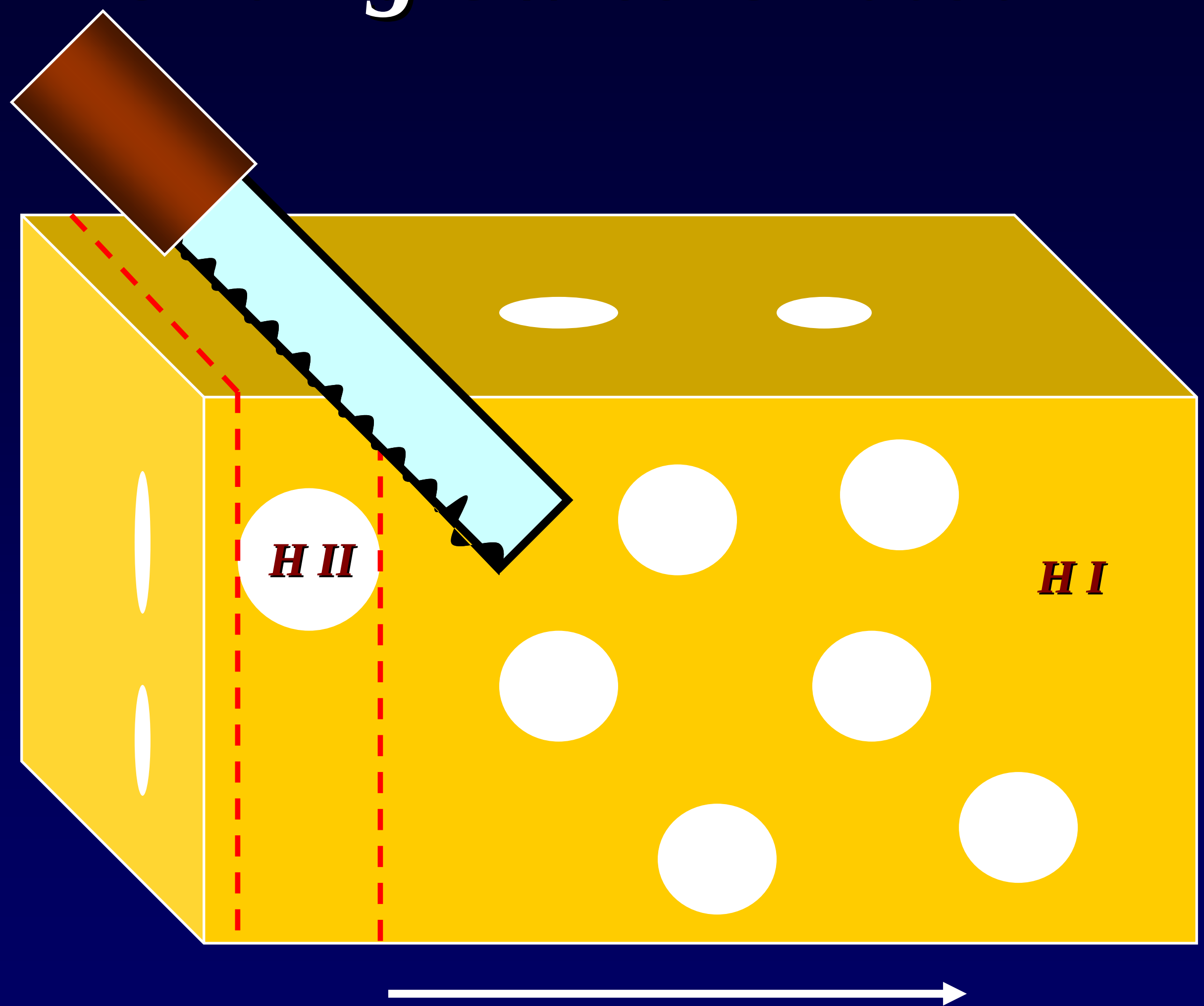

Observed wavelength ⇔ distance

21cm â (1 + z)

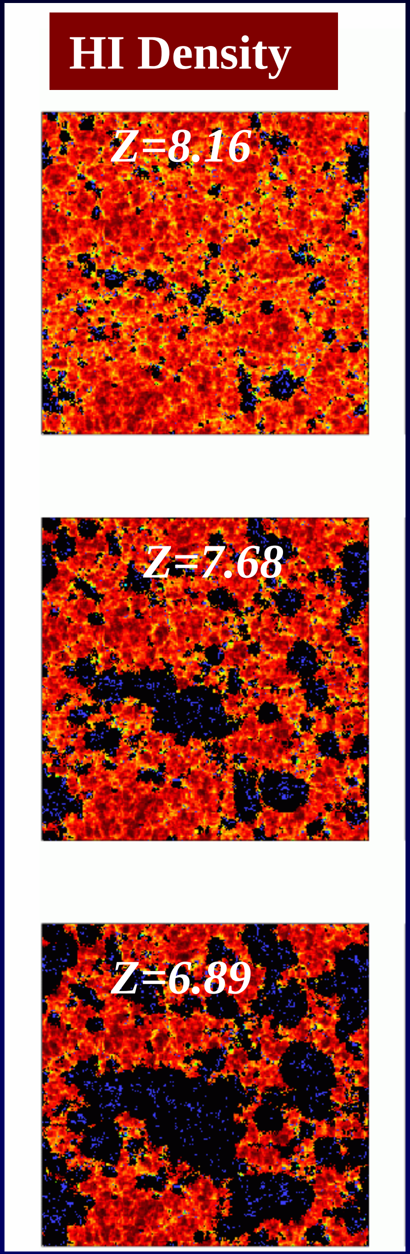

Zahn et al. 2006

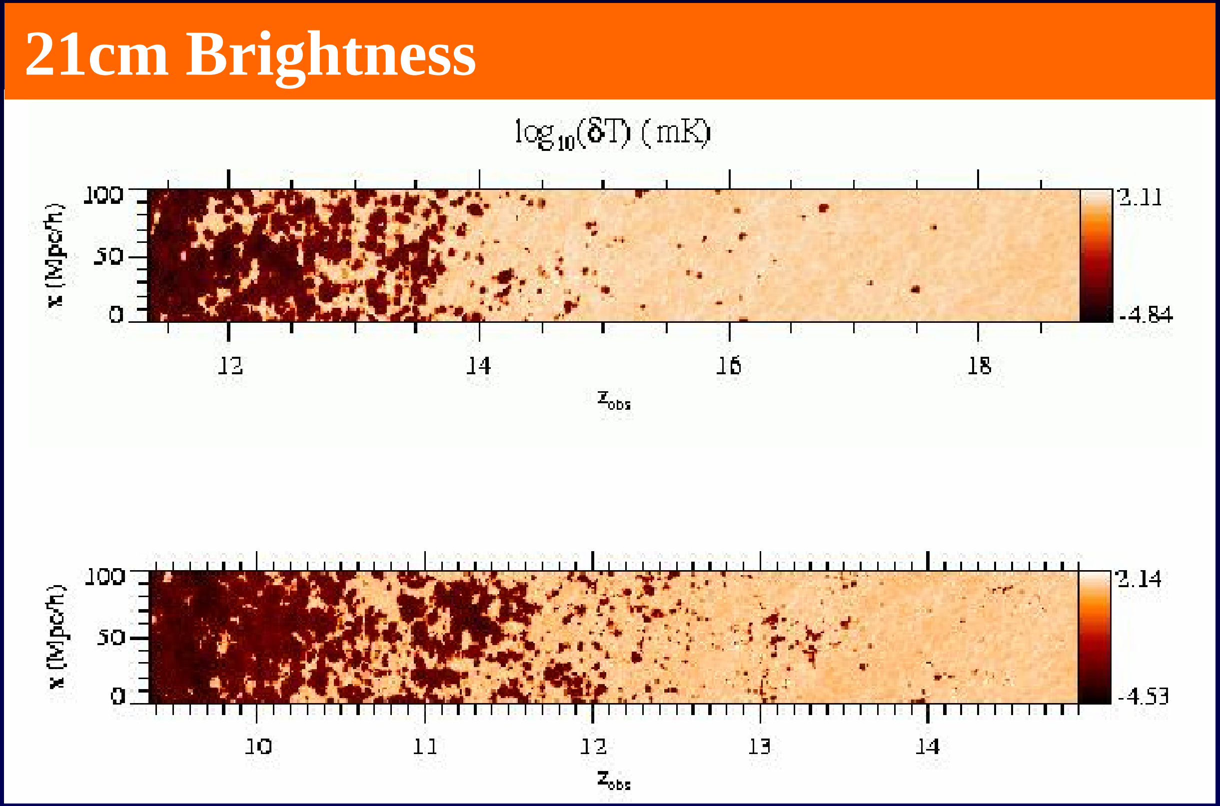

Mellema et al. 2006

Experiments

MWA (Mileura Wide-Field Array)

MIT/ATNF/CfA

LOFAR (Low-frequency Array)

Netherlands

21CMA (formerly known as PAST)

China

PAPER

UCB/NRAO

GMRT (Giant Meterwave Radio Telescope)

India/CITA/Pittsburg

SKA (Square Kilometer Array)

International

Mileura Wide-Field Array: *mapping cosmic hydrogen through its 21cm emission*




- 4mx4m tiles of 16 dipole antennae, 80-300MHz
- 500 antenna tiles with total collecting area 8000 sq.m. at 150MHz across a 1.5km area; few arcmin resolution

Primary challenge: foregrounds

- Terrestrial: radio broadcasting
- Galactic synchrotron emission
- Extragalactic: radio sources

(*Di-Matteo et al. 2004*)

$$N_\nu \sim 0.4\,\mathrm{mK}\left(\frac{I_\nu}{5\times10^5\mathrm{Jy\ sr^{-1}}}\right)\left(\frac{l_{\rm min}}{35}\right)\left(\frac{5000}{l_{\rm max}}\right)\left(\frac{0.016}{f_{\rm cover}}\right) \times\left(\frac{1\ \mathrm{year}}{t_0}\right)^{1/2}\left(\frac{\Delta\nu}{\nu}\right)^{-1/2}\left(\frac{50\ \mathrm{MHz}}{\nu}\right)^{5/2},$$

where $l_{\rm min}$ is the minimum observable l as determined by the field of view of the instruments, $l_{\rm max}$ is the maximum observable l as determined by the maximum separation of the antennae, $f_{\rm cover}$ is the fraction of the array area thats is covered by telescopes, t_0 is the observation time and $\Delta\nu$ is the frequency range over which the signal can be detected. The numbers adopted above are appropriate for the inner core of the *LOFAR* array (*http://www.lofar.org*), planned for initial operation in 2006.

Although the sky brightness (>10K) is much larger than the 21cm signal (<10mK), the foregrounds have a smooth frequency dependence while the signal fluctuates rapidly across small shifts in frequency (=redshift). Preliminary estimates indicate that the 21cm signal is detectable with the forthcoming generation of low-frequency arrays (Zaldarriaga et al. astro-ph/0311514; Morales & Hewitt astro-ph/0312437)

Power-Spectrum Sensitivity

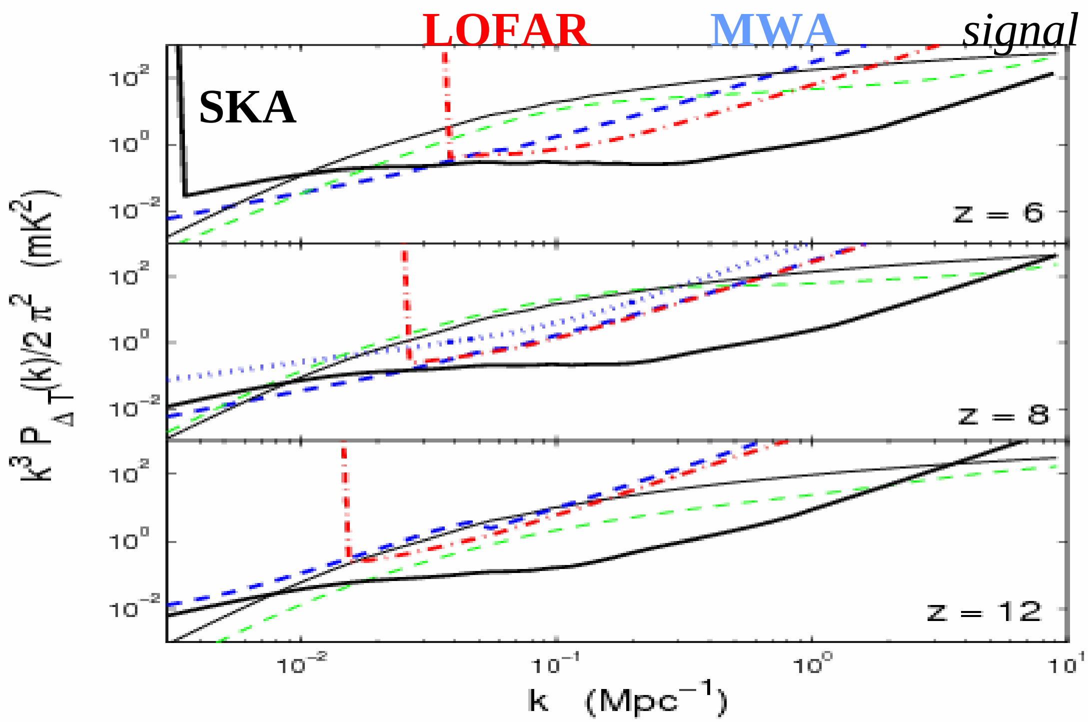

Isotropic power spectrum sensitivity, in logarithmic bins with $\Delta k = k/2$, for several experimental configurations. In each panel, the thin solid and dashed curves show estimates of the signal with and without reionization. The thick solid, dashed, and dot-dashed curves show error estimates for 1000 hour observations over 6 MHz with the SKA, MWA, and LOFAR, respectively. Each assumes perfect foreground removal. The dotted curve in the middle panel assumes a flat antenna distribution for the MWA. From ***McQuinn et al. 2006***

$$T_{\rm sky} \sim 180 \left(\frac{\nu}{180 \text{ MHz}}\right)^{-2.6} \text{K}$$

$$\Delta T^N|_{\rm int} \sim 2 \text{ mK} \left(\frac{A_{\rm tot}}{10^5 \text{ m}^2}\right)^{-1} \left(\frac{10'}{\Delta\theta}\right)^2 \left(\frac{1+z}{10}\right)^{4.6} \left(\frac{\text{MHz}}{\Delta\nu}\frac{100 \text{ hr}}{t_{\rm int}}\right)^{1/2}.$$

Observing the Stars

Hubble Ultra Deep Field (HUDF)

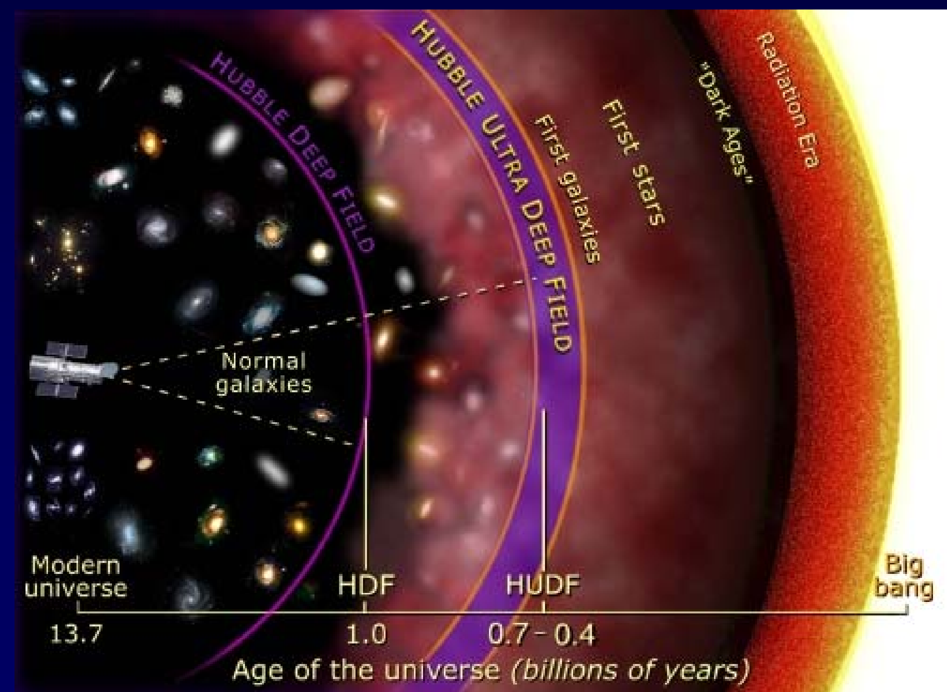

James Webb Space Telescope *(successor to* ***Hubble Space Telescope****)*: Searching for the First Light

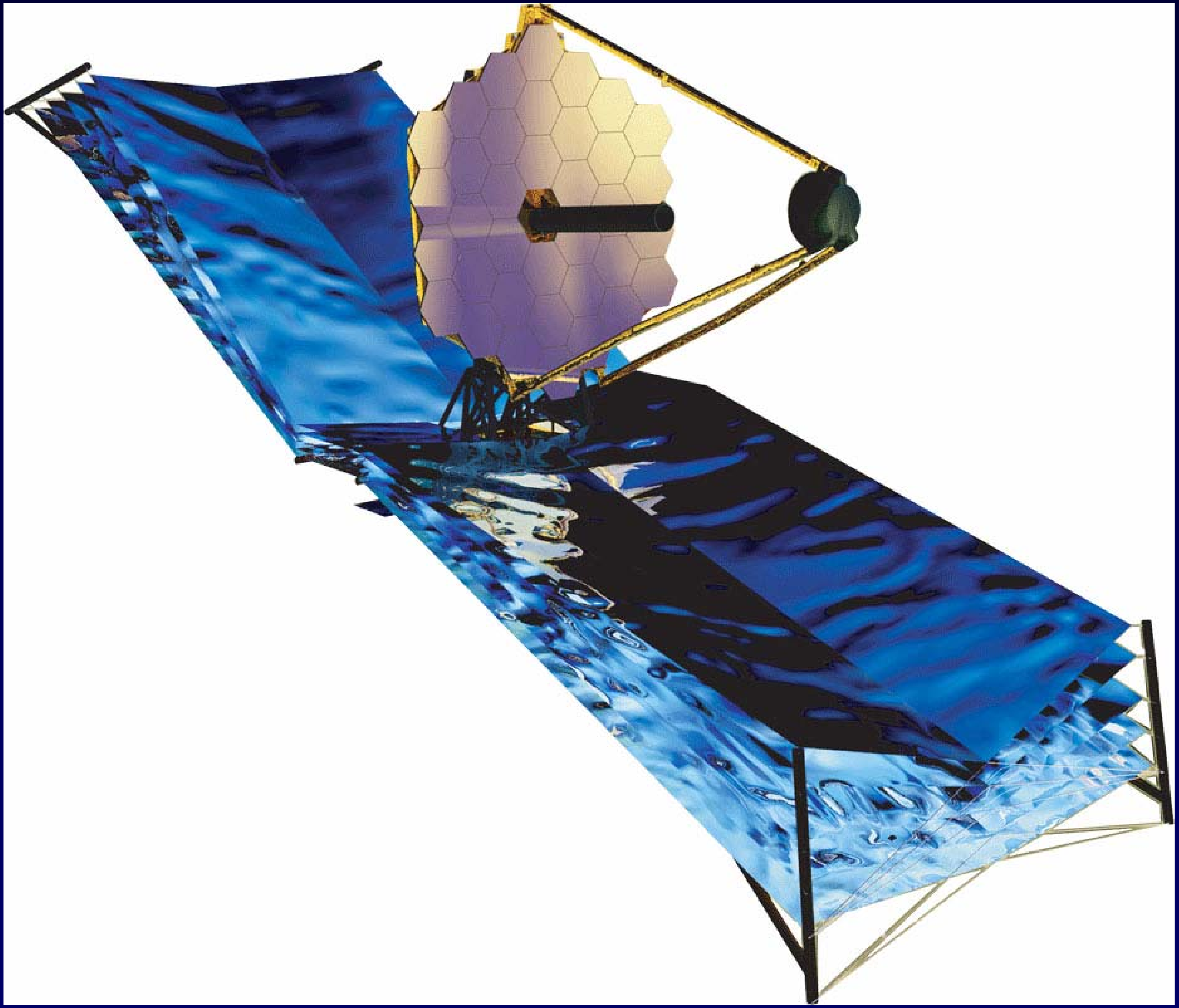

Mirror diameter: 6.5 meter

Material: beryllium

18 segments

Wavelength coverage: 0.6-28 micron

L2 orbit

Launch date: 2013

Extremely Large Telescopes (20-40 meters)

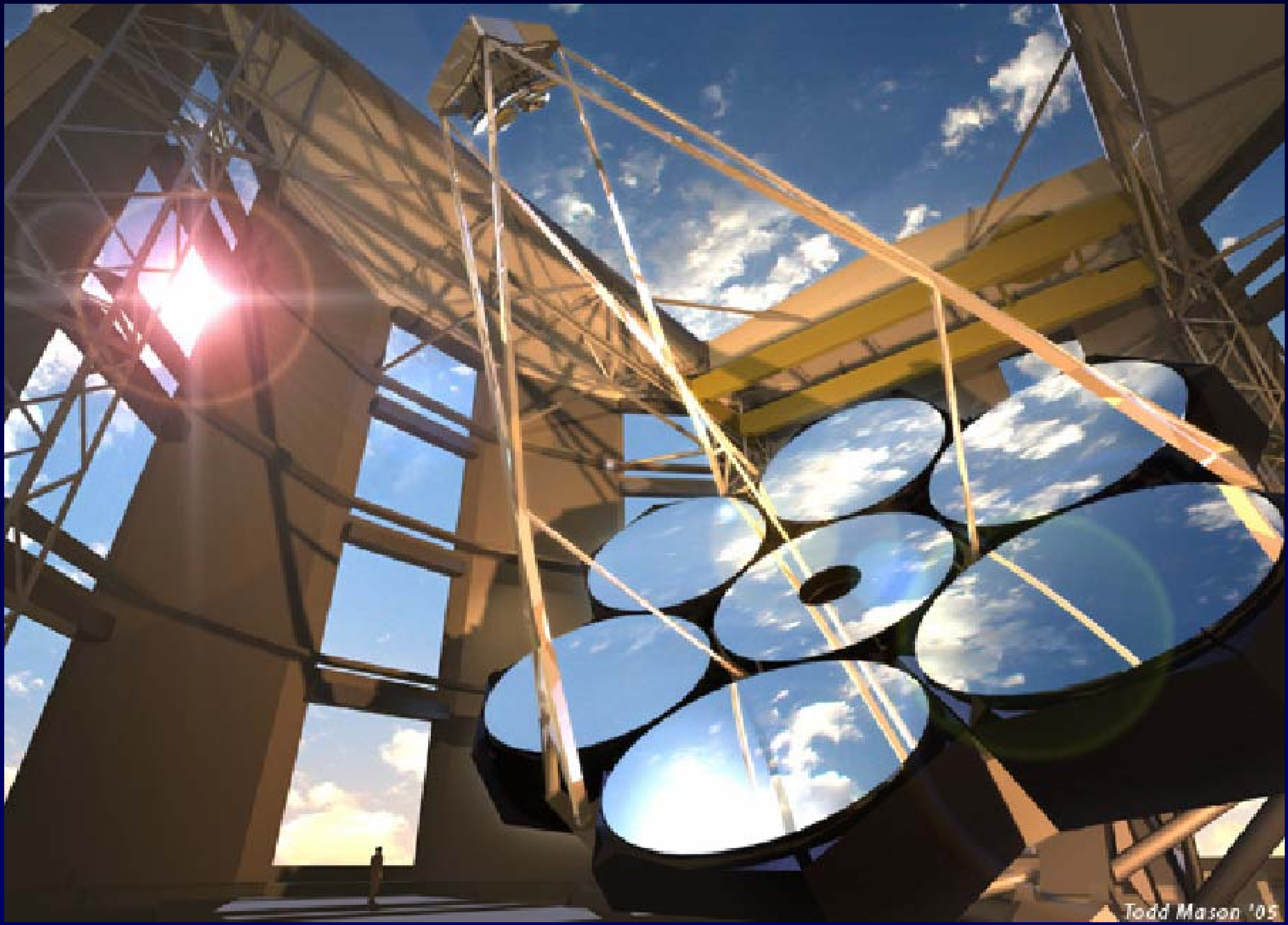

- GMT=Seven mirrors, each 8.4m in diameter
- TMT, EELT – segmented 20-40m aperture

Cross-correlation between 21cm brightness and galaxy density

Infrared imaging

21cm mapping

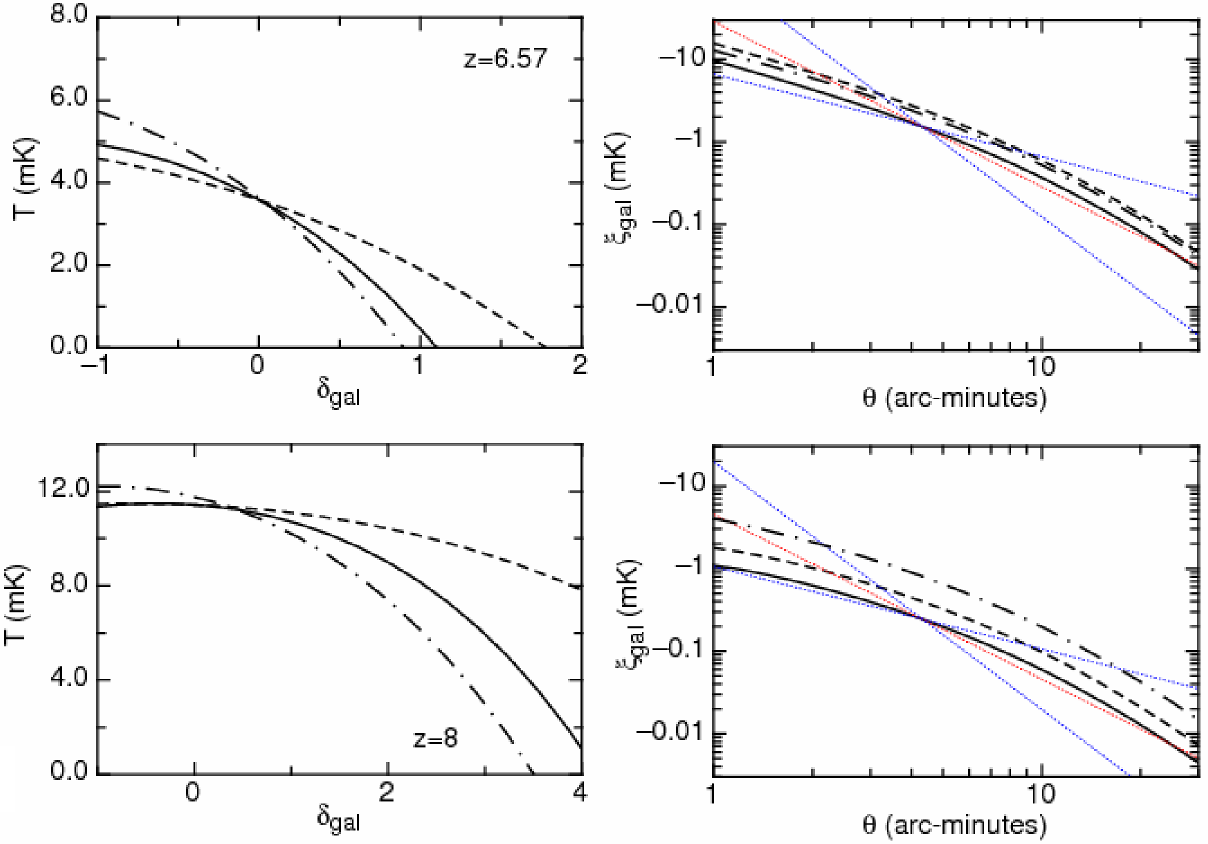

Figure 4. *Left*: 21cm brightness temperature as a function of $\delta_{\rm gal}$. Two values of galaxy mass are assumed for a clumping of $C = 10$, $M = 10^{10}M_\odot$ (solid line) and $M = 10^{11}M_\odot$ (dashed line). The dot-dashed line shows $C = 2$ with $M = 10^{10}M_\odot$. *Right*: The cross-correlation function $\xi_{\rm gal} = \langle\delta_{\rm gal}(T - \langle T\rangle)\rangle$ for the IGM smoothed on various angular scales (θ). The function is presented assuming $C = 10$ for masses of $M = 10^{10}M_\odot$ (solid line) and $M = 10^{11}M_\odot$ (dashed line). The dot-dashed line represents $C = 2$ with $M = 10^{10}M_\odot$. The lines show power-laws of slope $d(\log\xi_{\rm gal})/d(\log\theta) = -1$, -2 and -3. The upper and lower rows correspond to observations at $z = 6.57$ and $z = 8$ respectively.

Wyithe & Loeb (2006)

The Correlation Between Unresolved Star Formation and 21cm Emission During the Reionization Epoch

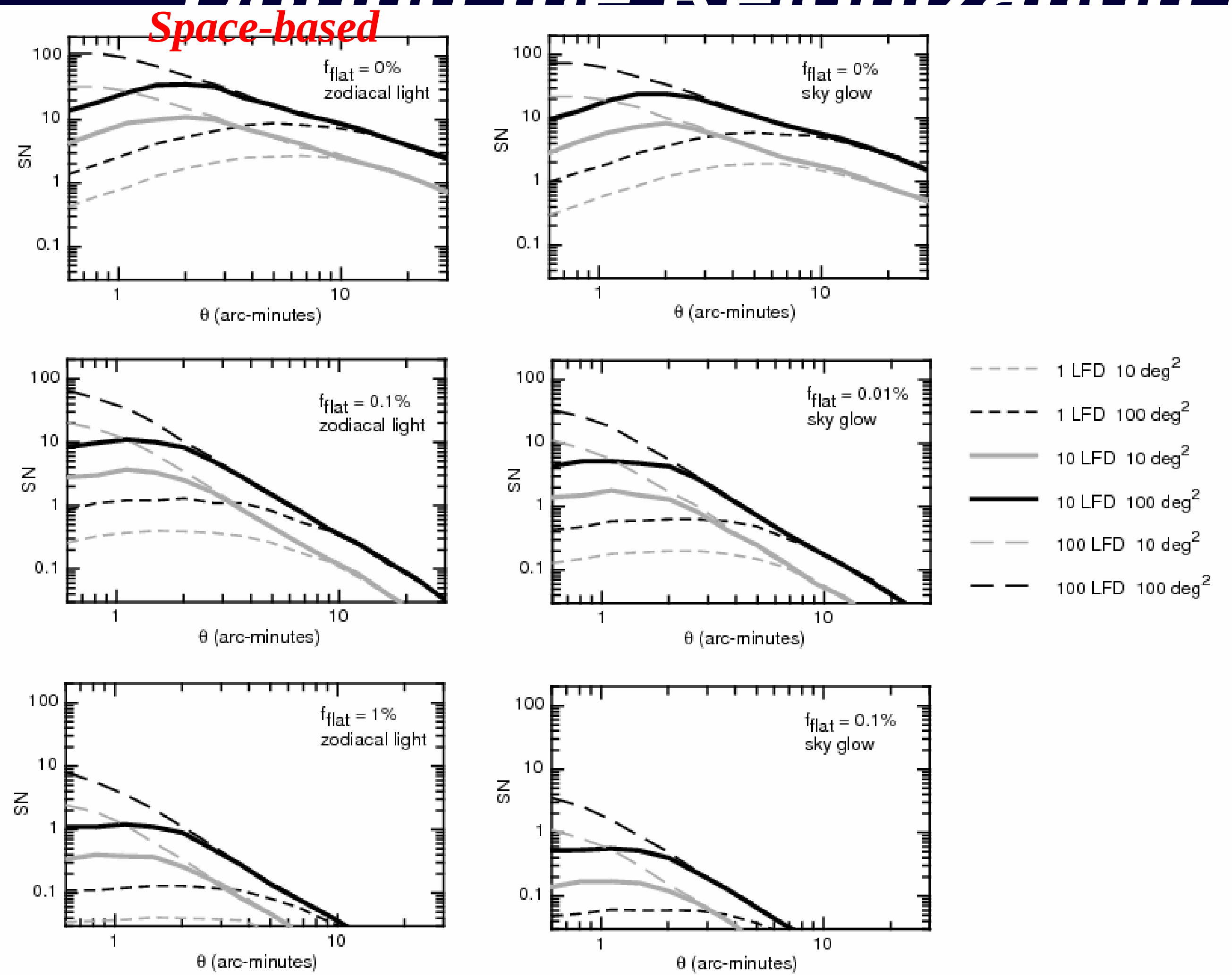

Figure 4. Signal to noise ratios as a function of angle. In each panel six cases are shown, corresponding to Lyα surveys with areas of $A = 10$ and 100 square degrees using a 2m telescope and a 1 hour integration; combined with low-frequency arrays of collecting area corresponding to 1, 10 and 100 LFDs with an integration time 1000 hours. The left-hand panels correspond to space based (i.e. no sky-glow, but including zodiacal light), and the right-hand panels to ground based near-IR observations (i.e. including sky glow). The value of $f_{\rm flat}$ is listed in each case. Note the assumed values for $f_{\rm flat}$ are an order of magnitude lower for ground based observations.

Wyithe, Loeb, & Schmidt 2007

Clustering of Lya Emitters

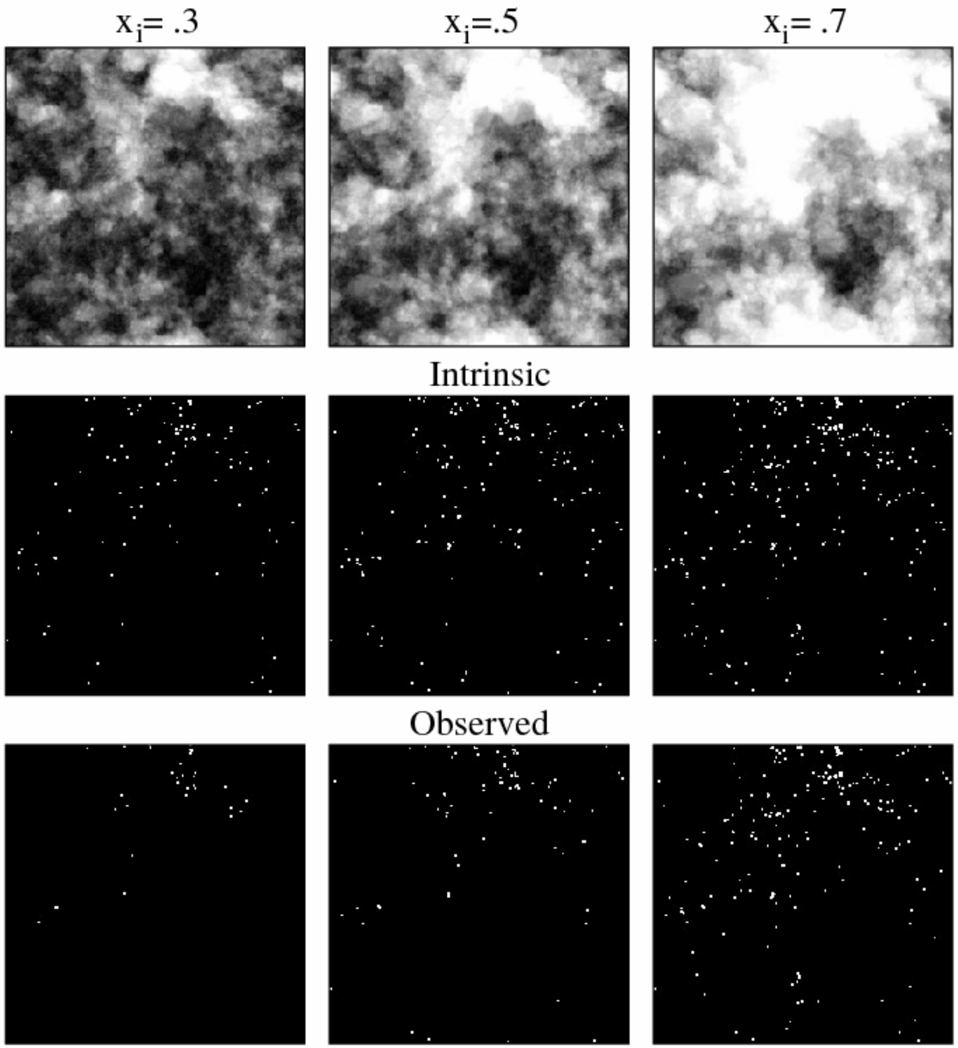

Figure 2. Top panels show the projection of $\bar{x}_i$ in the survey volume. In the white regions the projection is fully ionized and in black it is neutral. The left, middle, and right panels are for $z = 8.2$ ($\bar{x}_i = 0.3$), $z = 7.7$ ($\bar{x}_i = 0.5$), and $z = 7.3$ ($\bar{x}_i = 0.7$). The middle and bottom rows are the intrinsic and observed Lyα emitters maps, respectively, for $f_{\rm E} = 0.25$ and assuming that we can observe unobscured emitters with $m \exp(-\tau_\alpha(\nu_0)) > 7 \times 10^{10} M_\odot$. (Note that $L_{\rm int,E} \propto m$.) The observed distribution of emitters is modulated by the location of the HII regions (compare bottom panels with corresponding top panels). Each panel is 94 Mpc across (or 0.6 degrees on the sky), roughly the area of the current Subaru Deep Field (SDF) at $z = 6.6$ (Kashikawa et al. 2006). The depth of each panel is $\Delta\lambda = 130$ Å, which matches the FWHM of the Subaru 9210 Å narrow band filter. The number densities of Lyα emitters for the panels in the middle row are few times larger than the number density in the SDF photometric sample of $z = 6.6$ LAEs.

McQuinn et al.
arXiv:0704.2239

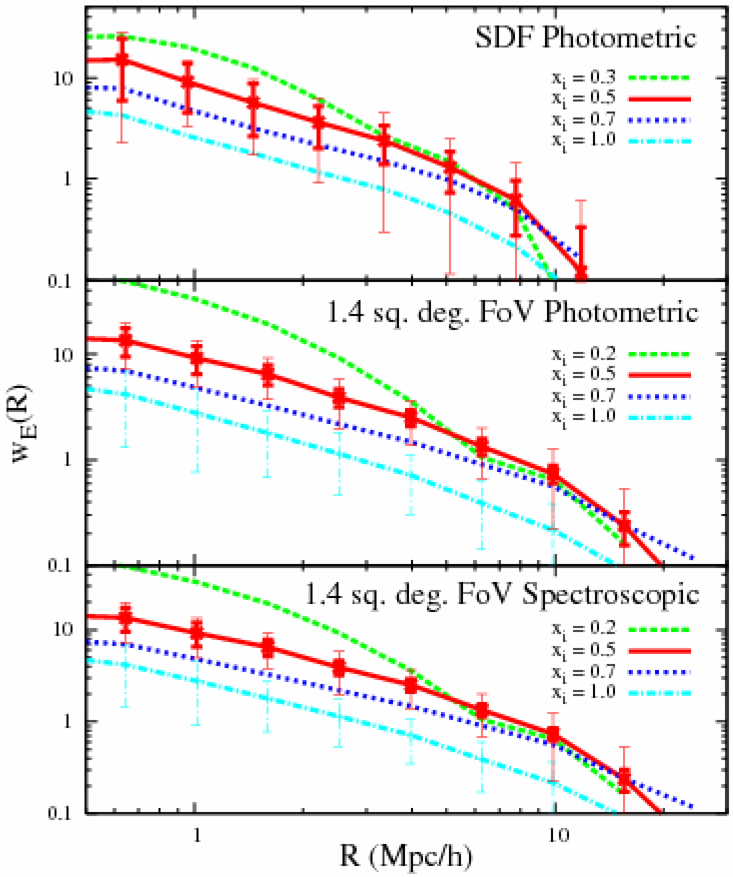

Figure 10. Angular correlation function of emitters at $z = 6.6$, assuming that observed emitters reside in halos with $m\ \exp(-\tau_\alpha(\nu_0)) > 7 \times 10^{10}\ M_\odot$. The curves in the top panel are calculated in the same volume and with the same number of emitters, 58, as the SDF photometric sample. The bottom two panels are in a volume a slightly larger volume than the upcoming 1 sq. deg. Subaru/XMM-Newton Deep Survey (SXDS), with 250 emitters in the middle panel and with 190 in the bottom one. The thick error bars owe to shot noise, and the thin owe to shot noise plus cosmic variance. To calculate these errors, we conservatively assume $F_c = 0.25$ in the top two panels ($F_c = 0$ in the bottom panel). Current surveys can potentially distinguish an ionized universe (the curves labeled "intrinsic") from a universe with $\bar{x}_i \lesssim 0.5$.

From the Subaru Deep Field at z=6.6

xn< 0:5at2 à û

But subject to uncertianties due to detailed radiative transfer effects: see Dijkstra et al, arXiv:astro-ph/0701667

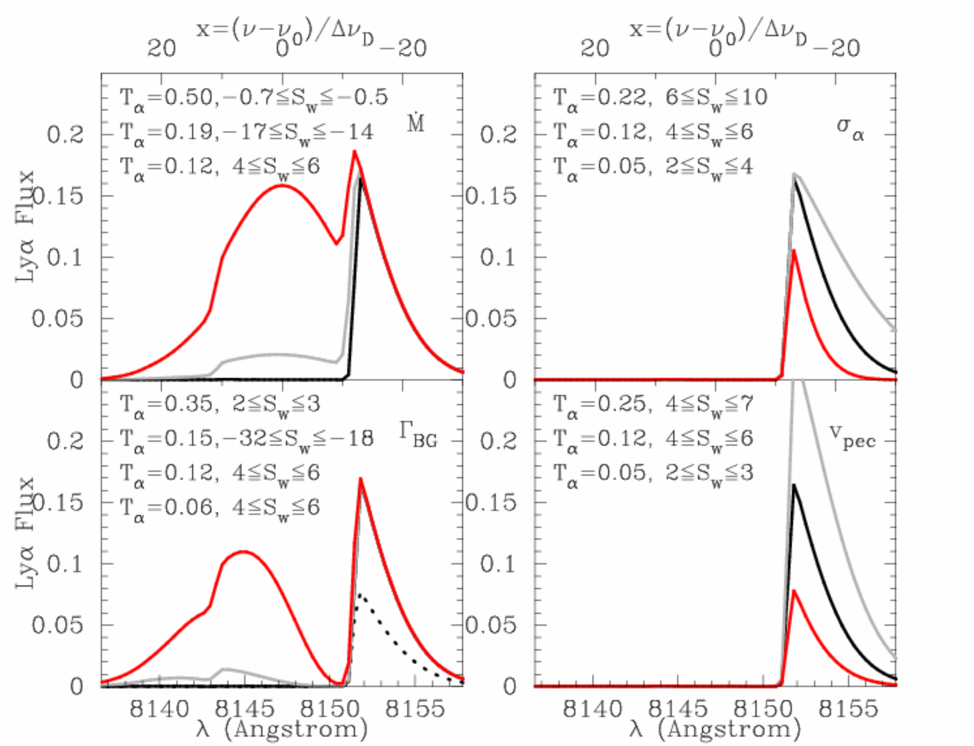

Figure 4. The observed Lyα line from $z = 5.7$ galaxies in a reionised IGM for a range of different models. The upper right corner o each panel shows the model-parameter that is varied. *Top Left:* $\dot{M}_* = 10 M_\odot/\mathrm{yr}$ (*black*), $\dot{M}_* = 10^2 M_\odot/\mathrm{yr}$ (*grey*) and $\dot{M}_* = 10^3 M_\odot/\mathrm{y}$ (*red*). *Top Right:* $\sigma_\alpha = 1.0 v_{\rm circ}$ (*black*), $\sigma_\alpha = 0.7 v_{\rm circ}$ (*red*) and $\sigma_\alpha = 1.5 v_{\rm circ}$ (*grey*). *Lower Left*: Variation of the ionising background: no ionising background (*dotted*), $\Gamma_{\rm BG}$(*black*), $10\Gamma_{\rm BG}$ (*grey*) and $100\Gamma_{\rm BG}$ (*red*). *Lower Right*: Impact of galaxies peculiar velocity: $v_{\rm pec} =$ (*black*), $v_{\rm pec} = -0.5\sigma_\alpha$ (*red*) and $v_{\rm pec} = 0.5\sigma_\alpha$ (*grey*). For each model the total transmission, T_α and the skewness of the line, S_W, ar shown.

The Imprint of Reionization on Galaxy Clustering

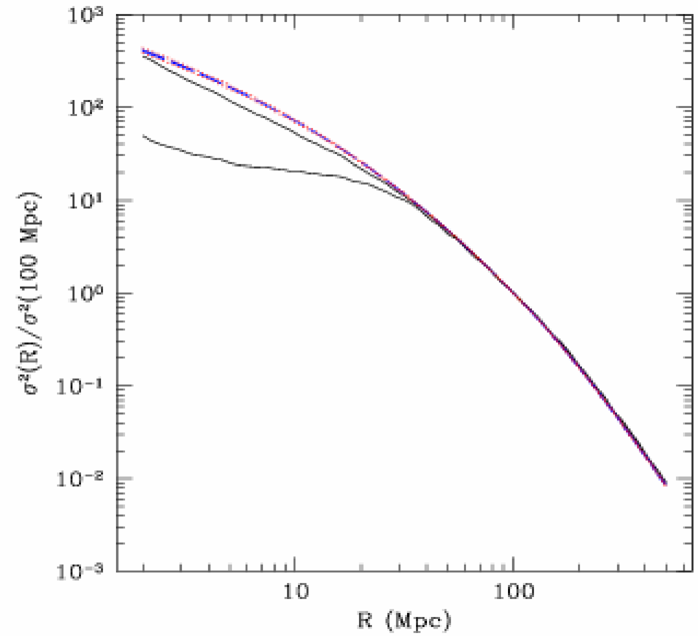

FIG. 5.— The normalized $\sigma^2(R)$ for $z_R = 15$ and $z_R = 6$ (upper and lower solid black curves, respectively); the limiting cases of the best current constraints of n (red, dotted curves) and α (blue, dashed curves).

Inhomogeneous photo-ionization heating to ø 10^4K ***modulates the minimum mass of galaxies on scales of tens of comoving Mpc***

Babich & Loeb 2006, ApJ, 640, 1

The Imprint of Reionization on Galaxy Bias

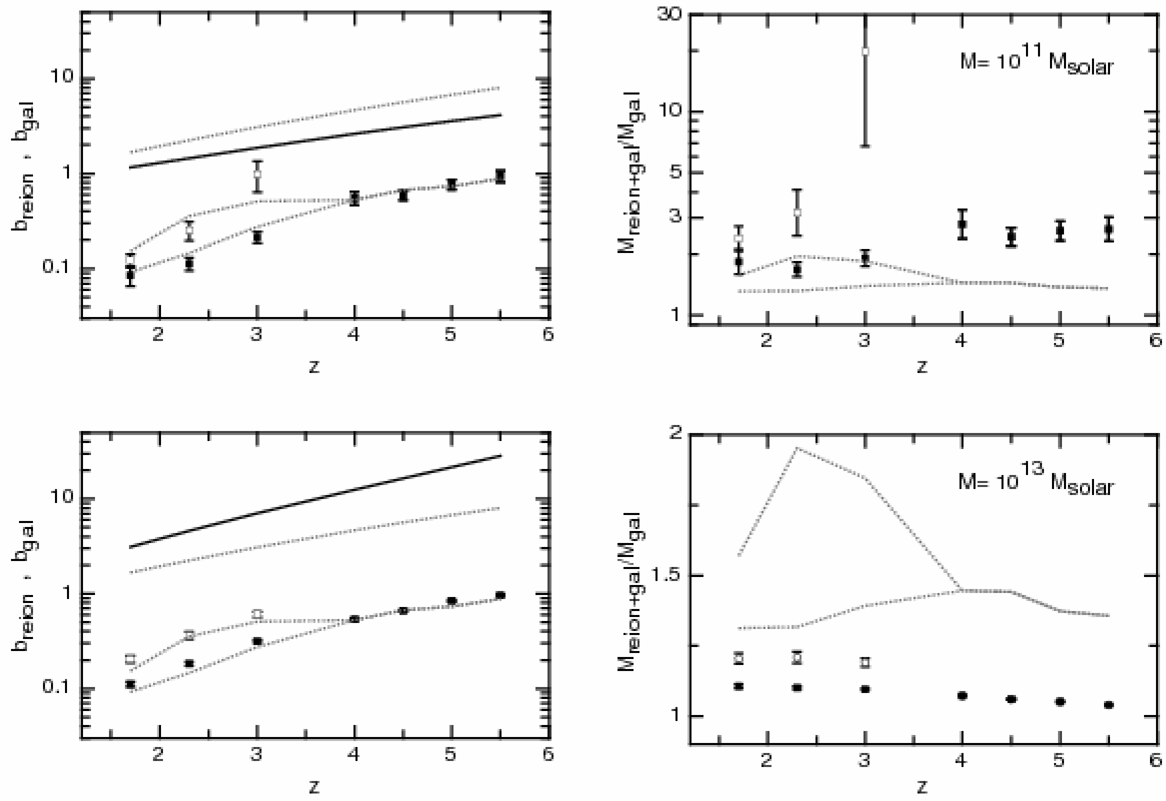

Figure 3. Examples of clustering bias in Ly-break galaxies induced by reionization as a function of the halo mass. *Left Hand Panels:* The bias introduced by reionization in cases where helium reionization at $z \sim 3.5$ is considered in addition to hydrogen reionization (open squares) and where it is not (solid squares). The bias was computed assuming a flux evaluated at a rest-frame wavelength of $1350\AA$ within a $400\AA$ window. The galaxy bias is shown by the solid line for comparison. The error bars represent the statistical noise in the simulations due to the finite number of merger trees. *Right Hand Panels:* The factor by which the mass will be overestimated in clustering analyses where reionization is not considered. Results are shown for two halo masses, $M = 10^{11} M_\odot$, and $M = 10^{13} M_\odot$. In each case the corresponding results for $M = 10^{12} M_\odot$, as presented in Figure 2, are shown for comparison (light lines).

Because of the modulation in the minimum galaxy mass, gas is converted into stars later in overdense regions (reionized earlier)

Wyithe & Loeb, arXiv:0706.3744

Implications for the Cosmic Reionization from the Optical Afterglow Spectrum of the Gamma-Ray Burst 050904 at $z = 6.3$*

Tomonori TOTANI[1], Nobuyuki KAWAI[2], George KOSUGI[3], Kentaro AOKI[4], Toru YAMADA[3]
Masanori IYE[3], Kouji OHTA[1], and Takashi HATTORI[4]

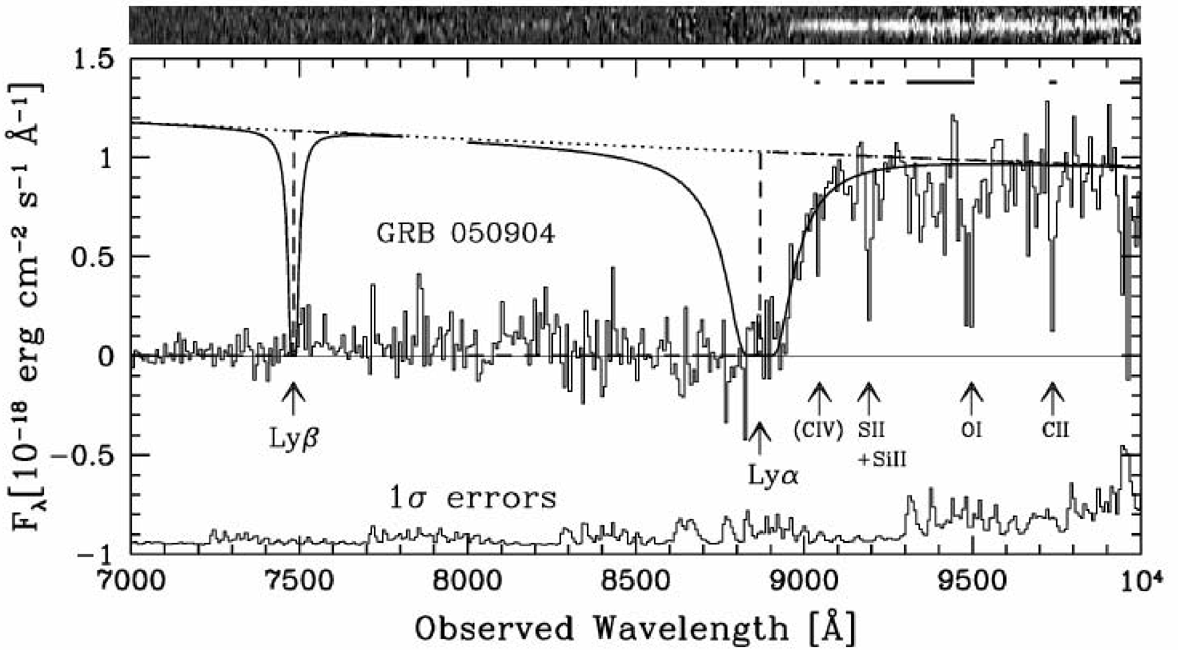

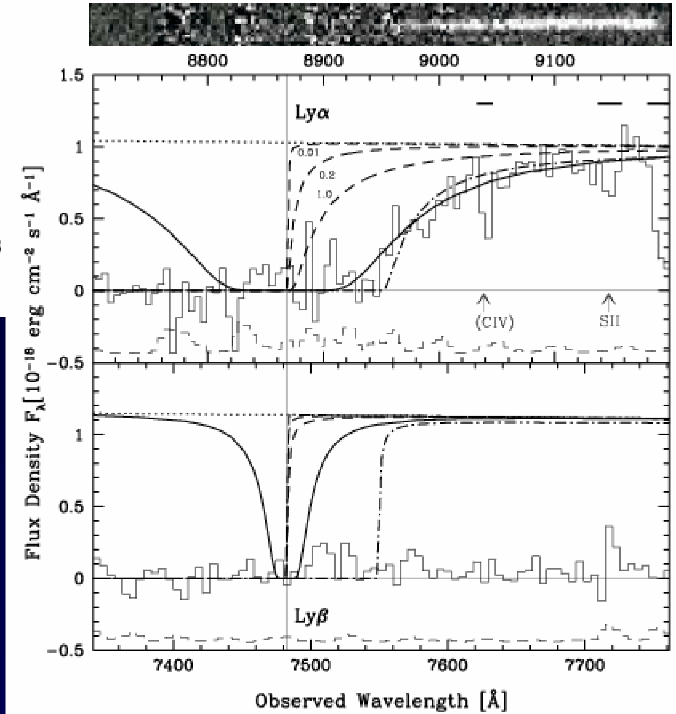

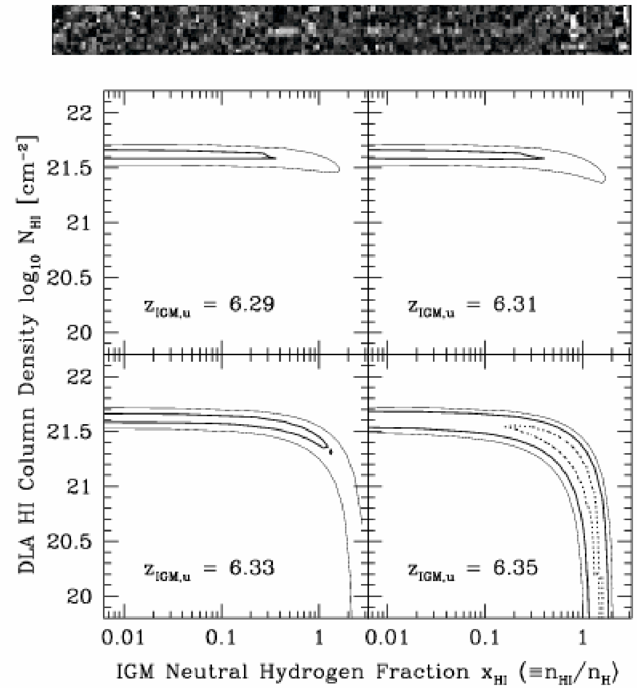

Enough about the past…
what does the future hold?

The Long Term Future of Extragalactic Astronomy

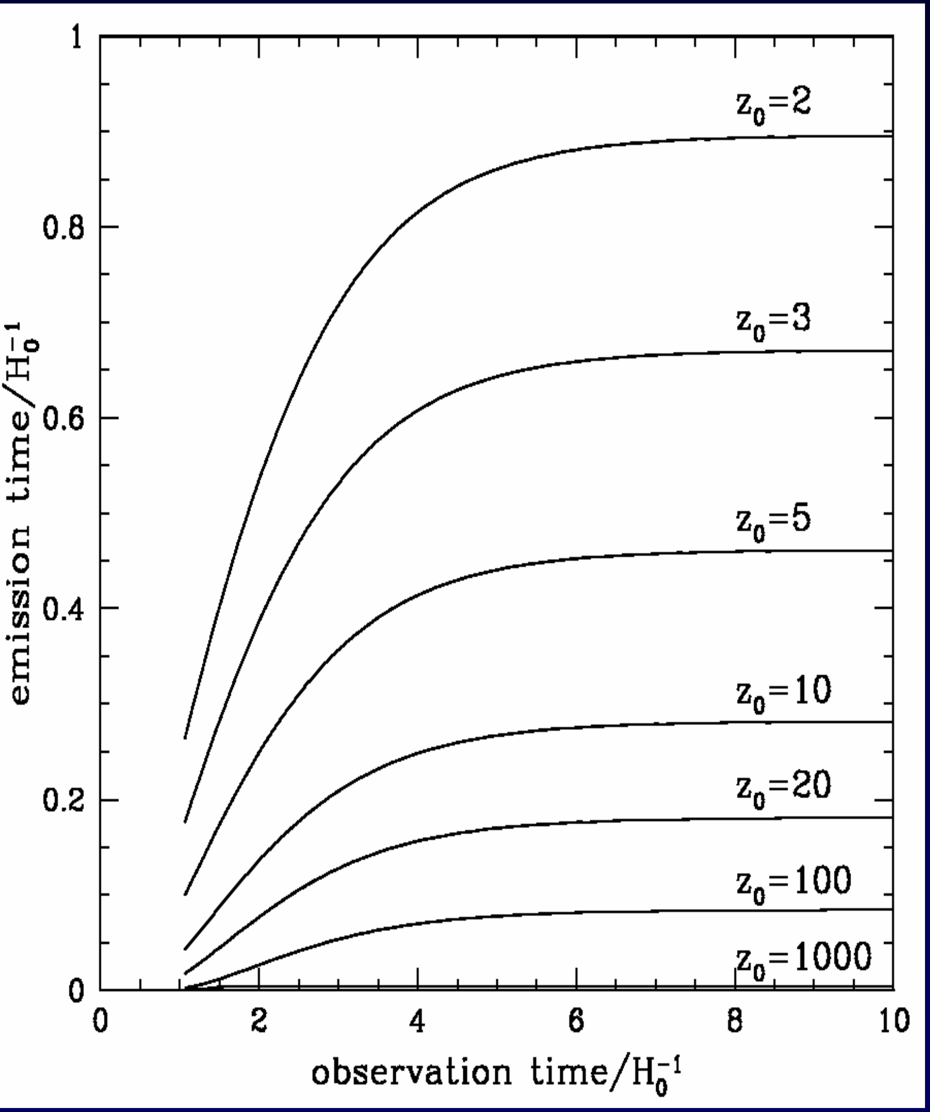

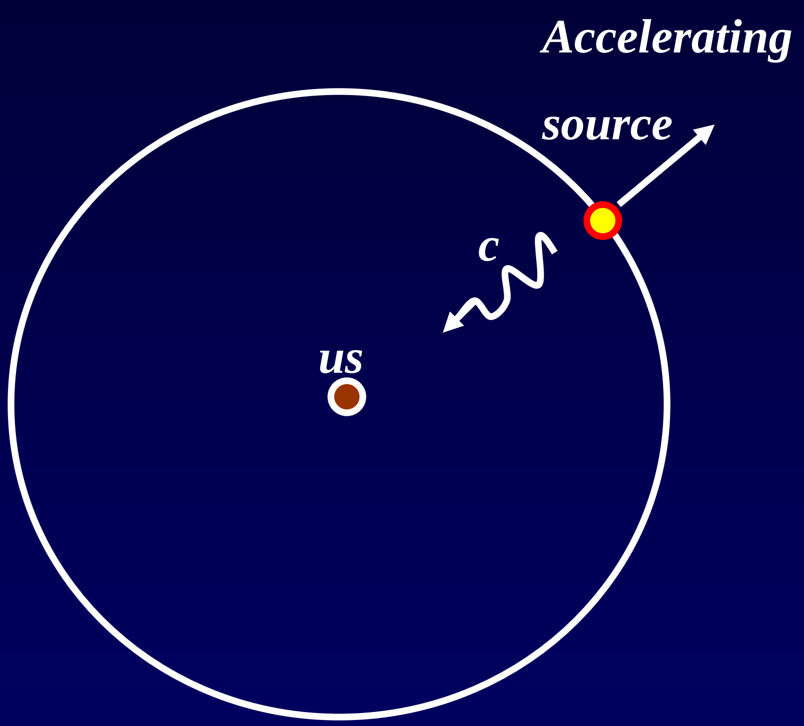

All galaxies beyond a redshift of z=1.8 are already outside our horizon (no cell phone communication to z>1.8!). (Loeb 2001)

How many galaxies will reside within our event horizon in 100 billion years?

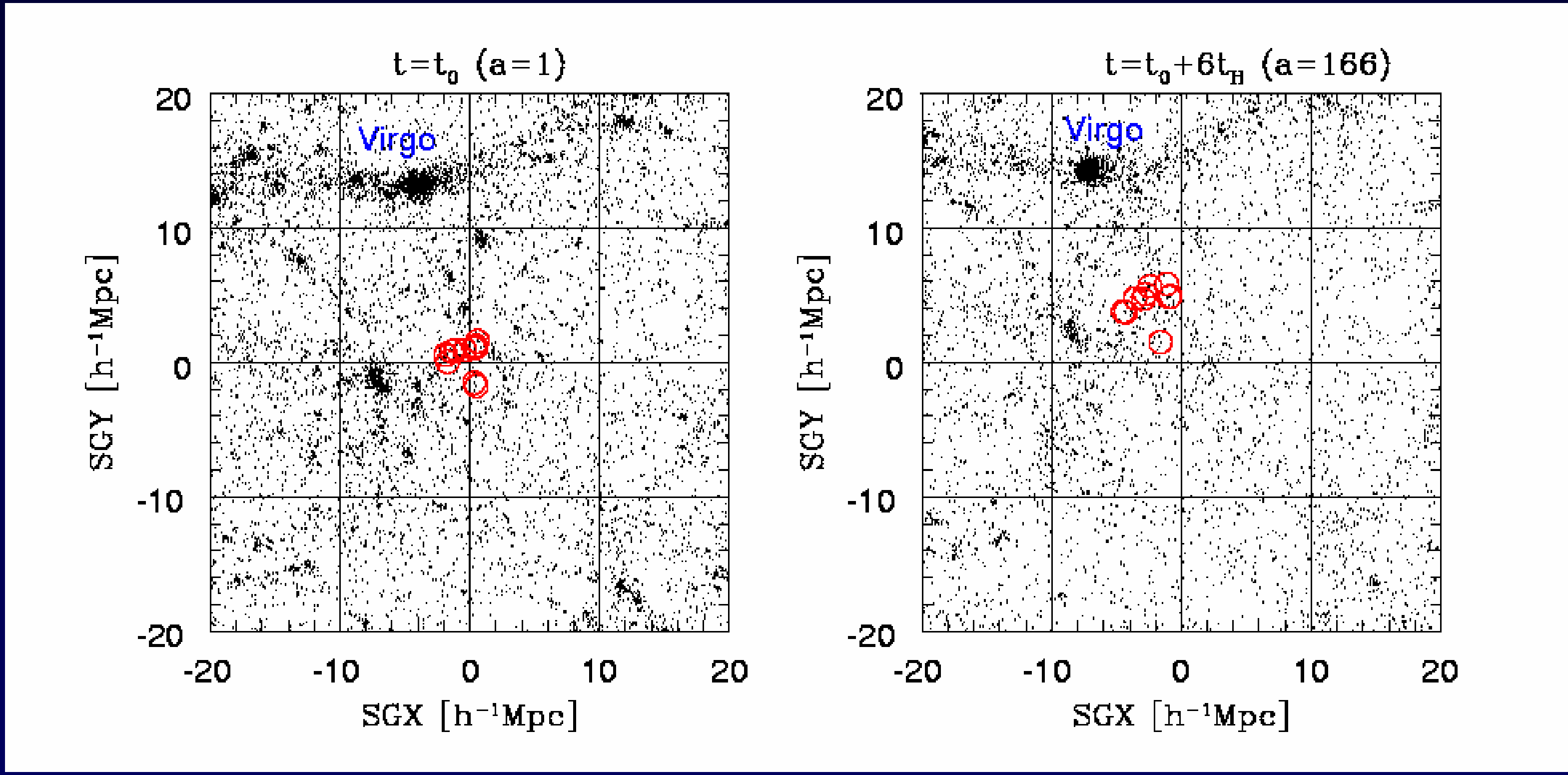

Answer: ***one surrounded by vacuum***

The merger product of the Andromeda and Milky-Way

The Forthcoming Collision Between the Milky-Way and Andromeda

- The merger product is the only cosmological object that will be observable to future astronomers in 100 billion years
- Collision will occur during the lifetime of the sun,
- The night sky will change
- Simulated with an N-body/hydrodynamic code (Cox & Loeb 2007)
- ***The only paper of mine that has a chance of being cited in five billion years…***

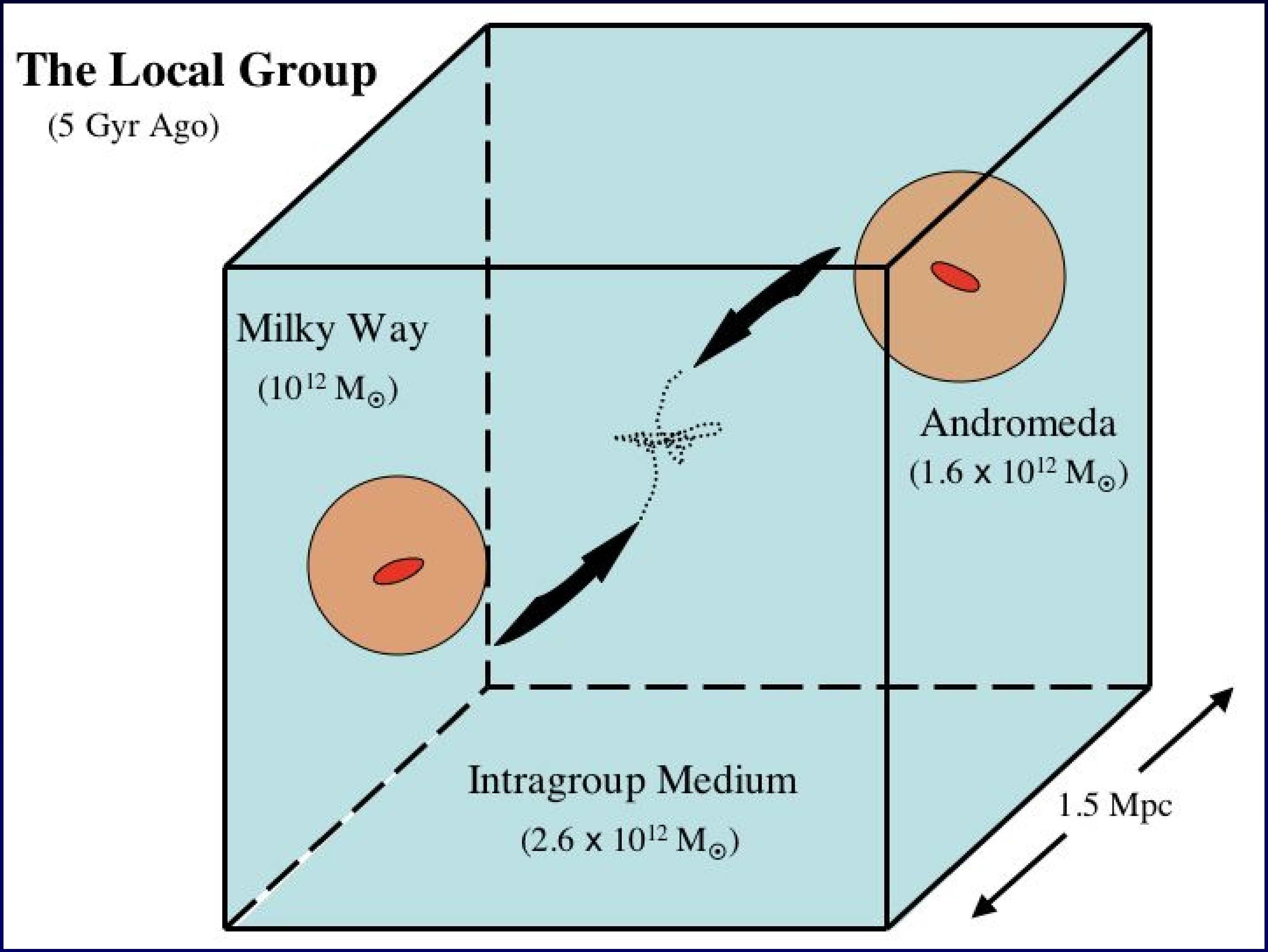
The Local Group
(5 Gyr Ago)
Milky Way
(10^12 M_⊙)
Andromeda
(1.6 x 10^12 M_⊙)
Intragroup Medium
(2.6 x 10^12 M_⊙)
1.5 Mpc

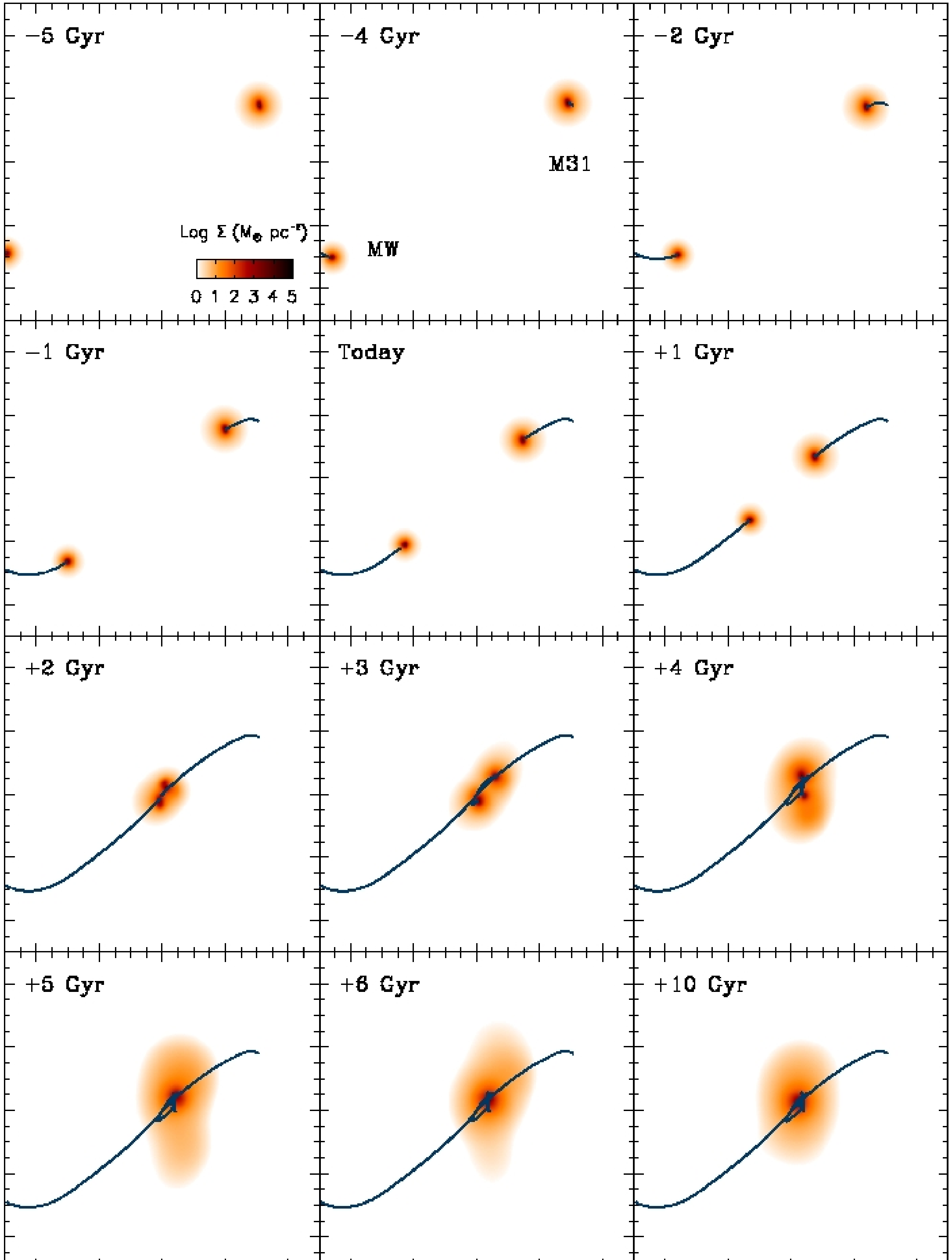
−5 Gyr
Log Σ (M☉ pc⁻²)
0 1 2 3 4 5
−4 Gyr
M31
MW
−2 Gyr
−1 Gyr
Today
+1 Gyr
+2 Gyr
+3 Gyr
+4 Gyr
+5 Gyr
+6 Gyr
+10 Gyr

The Future Collision between the Milky Way and Andromeda Galaxies

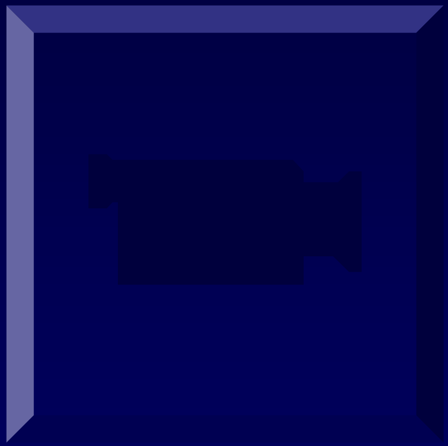

The Last Billion Years of Star Formation in the Visible Universe

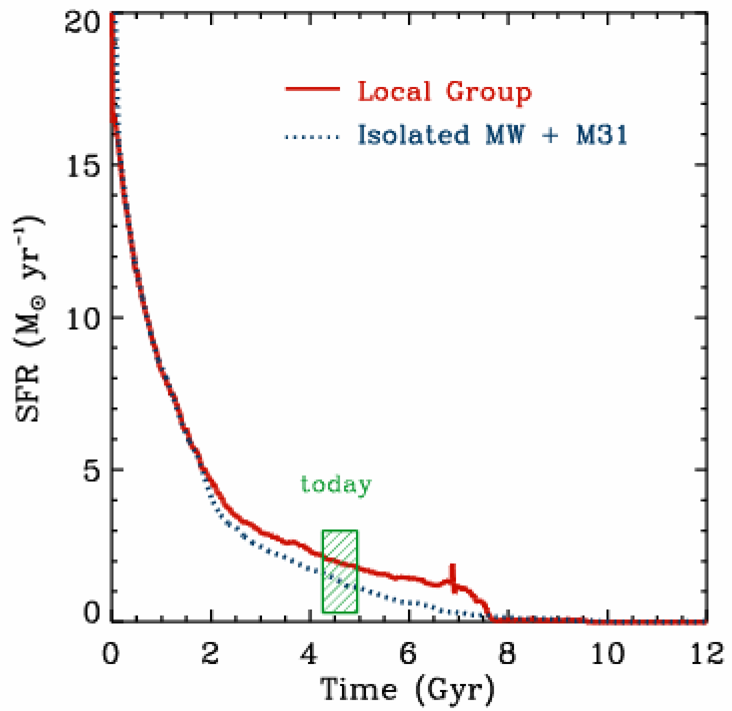

Figure 9. The cumulative star-formation rate during the merger of the Milky Way and Andromeda compared to the star formation for models of the Milky Way and Andromeda evolved in isolation.

Summary

- *21cm brightness fluctuations are expected to be anti-correlated with infrared galaxies during reionization*
- *Lya galaxies should show excess clustering due to a neutral IGM (but subject to radiative transfer effects in the infall region around them)*
- *Light from unresolved Lya galaxies should also be anti-correlated with 21cm fluctuations but its detection is challenging*
- *Reionization leaves an imprint on the clustering of star-forming galaxies at intermediate redshifts. This compromises the use of galaxy surveys for precision cosmology (e.g. inflation,acoustic oscillations/dark energy).*